UNIVERSITÀ DEL PIEMONTE ORIENTALE

School of Medicine

Department of Health Sciences

Master degree in Medical Biotechnologies

Laboratory of Immunomics

(Centre for Translational Research on Autoimmune and Allergic Diseases - CAAD)

Immunophenotypic Signatures in Amyotrophic Lateral Sclerosis: From Peripheral Biomarker Discovery to Optimization of a High-Dimensional Cytometric Panel

Relator:

Dr. Davide Raineri

Supervisor:

Sara Nembrini

Candidate:

Pietro Manfredi

Matricula Number:

20063393

Academic year 2025-2026

Summary

Abstract

Amyotrophic lateral sclerosis (ALS) is a complex neurodegenerative disorder characterized by progressive upper and lower motor neuron loss, marked clinical heterogeneity, and a lack of specific diagnostic and prognostic biomarkers. Due to altered blood-brain barrier permeability, circulating immune cells infiltrate the neuronal space, yet their precise pathophysiological role in modulating disease kinetics remains poorly understood. Concurrently, identifying reliable, blood-based immunophenotypic biomarkers represents an urgent clinical need to improve diagnosis and patient stratification. To address these challenges, the study was structured in two sequential phases: first, to identify candidate prognostic and diagnostic immunophenotypic signatures via high-dimensional unsupervised analysis of peripheral blood from ALS patients; second, to design, optimize, and validate a highly sensitive flow cytometry panel, establishing a standardized methodological framework to deeply characterize the targeted populations identified in the first phase.

To discover novel candidate biomarkers, phase one employed a broad, unsupervised 19-color flow cytometry analysis on whole blood from 24 ALS patients and 15 healthy controls. This screening successfully revealed a statistically significant expansion of peripheral basophils ($CD123^+$ $HLA\text{-}DR^-$) in ALS patients versus controls ($p<0.05$). Furthermore, patient stratification by progression rate demonstrated that slow progressors exhibited significantly higher levels of basophils and classical monocytes ($CD14^+$ $CD16^-$), alongside a marked reduction in $CD4^+$ naïve T cells, compared to fast progressors ($p<0.05$).

Driven by the biological relevance of these findings, phase two focused on the technological development of the 22-color flow cytometry panel in order to deeply study the biology of the basophils. Developed through rigorous antibody titration to ensure methodological standardization, the protocol was further optimized to overcome technical challenges associated with tracking rare cell populations and preventing IgE cross-interference. This dedicated tool successfully resolved seven non-mutually exclusive basophil subsets defined by immediate (CD203c, CD13, CD164), intermediate (CD63, CD107b), and delayed (CD69) activation and degranulation kinetics.

In conclusion, this study bridges an initial immunophenotypic discovery with targeted methodological innovation. The identification of a distinct peripheral immune profile that directly correlates with the rate of disease progression provides new insights into ALS systemic cellular heterogeneity. Ultimately, the optimized 22-color panel delivers a robust, validated technical tool. Its future translation to large patient cohorts will be essential to track altered basophil kinetics, dissect their specific involvement in ALS physiopathology, and evaluate their concrete utility as novel, minimally invasive biomarkers.

Introduction

Amyotrophic Lateral Sclerosis Overview

Amyotrophic lateral sclerosis (ALS) is a rare neurodegenerative disorder of adulthood, characterized by the progressive involvement of lower motor neurons (LMN) and upper motor neurons (UMN). The degeneration of these specific neuronal populations disrupts the communication between the central nervous system and skeletal muscles, leading to progressive denervation, muscle atrophy and, ultimately, respiratory failure. Notwithstanding the common endpoint of motor neuron degeneration, the pathophysiological mechanisms underlying ALS are complex and not yet fully elucidated. As reviewed by Hu and colleagues, rather than a single causative factor, motoneuronal death is likely the result of the interaction among various environmental, genetic, and molecular factors. Together, these factors can trigger neurotoxicity through various proposed mechanisms (Figure 1), including glutamate excitotoxicity, abnormalities in both mitochondrial structure and function, impaired RNA metabolism and DNA repair, protein accumulation within the cytoplasmic environment and axonal transport defects (Hu et al., 2024).

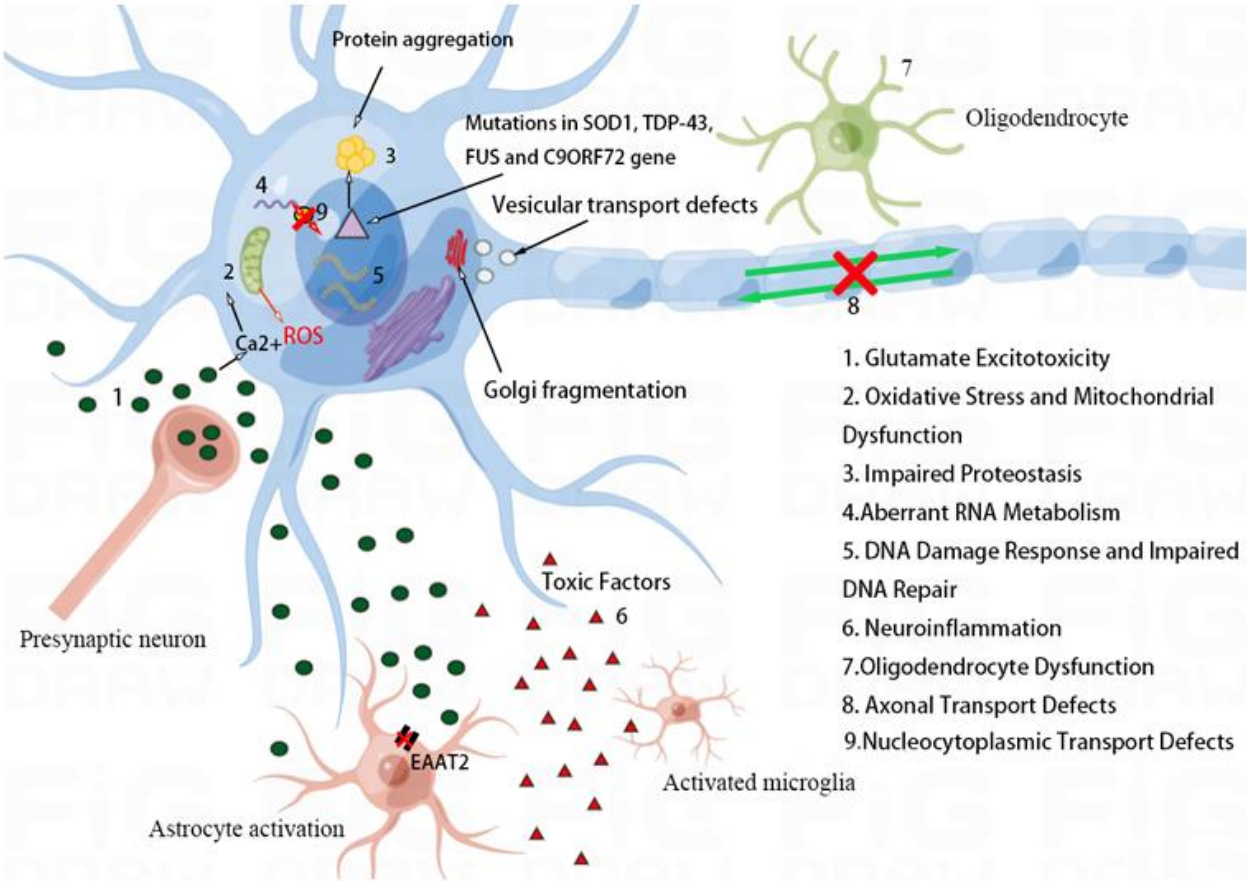

Figure 1: possible proposed mechanisms leading to motoneuron death characteristic of ALS pathology. (Hu et al., 2024)

Approximately 85-90% of cases are classified as sporadic ALS (sALS), arising from a combination of environmental factors and genetic susceptibility. The remaining 5-10% of cases are defined as familial ALS (fALS), linked to mutations in specific genes. Among these, the most frequently identified are mutations in *TARDBP* (encoding TDP-43), C9orf72, *SOD1*, and *FUS* (Goutman et al., 2022a). Crucially, the formation of intracellular aggregates containing TDP-43 represents the pathological hallmark in over 95% of all ALS cases. The displacement of this protein from the nucleus to the cytoplasm and its subsequent ubiquitination and phosphorylation are thought to trigger a feed-forward cycle of proteotoxicity and neurodegeneration (Neumann et al., 2006). Interestingly, certain mutations (e.g. *C9orf72* repeat expansions and FUS mutation) are strongly associated with rapid disease progression and short survival, whereas other variants (e.g. SOD1 mutations) are equally frequent in both slow and fast progressors (Witzel et al., 2022).

Beyond differences in neurotoxic mechanisms and progression rate, ALS is a highly heterogeneous disease also regarding its clinical manifestation. As reported by Chiò et al. (2011), spinal and bulbar onsets are the most frequent, whereas flail arm, flail leg, pyramidal, respiratory onset, pure lower motor neuron (PLMN), and pure upper motor neuron (PUMN) phenotypes are rarer. Although ALS generally exhibits a higher frequency in men than in women (1.29:1), different phenotypes show distinct gender distributions. For instance, while classic and flail arm phenotypes are more prevalent in men (1.65:1 and 4.00:1, respectively), other phenotypes, such as bulbar or flail leg, show a more balanced distribution (0.98:1 and 1.03:1, respectively) (Chiò et al., 2011).

Moreover, ALS symptoms extend beyond motor neuron degeneration and muscular atrophy. As reported by Beeldman et al. (2020), cognitive and behavioral decline are widespread features of ALS that emerge even during early symptomatic stages, affecting more than one-third of patients. This impairment is independent of physical or respiratory deterioration and highlights the early relevance of frontotemporal dysfunction within the ALS syndrome. Crockford et al. (2018) further demonstrated that this decline is localized to specific cognitive domains, particularly verbal fluency and executive functions. Conversely, non-specific functions, such as memory and visuospatial skills, do not show a significant correlation with disease progression. In addition, metabolic alterations are often observed in association with the pathology. ALS patients often exhibit hypermetabolism and mitochondrial dysfunction, leading to a loss of muscle mass and subcutaneous fat. Paradoxically, a redistribution of fat toward the visceral area is observed. Hypercholesterolemia is also common and frequently associated with longer survival and better respiratory function (Ahmed et al., 2016). Consequently, ALS is increasingly recognized as a systemic syndrome where metabolic shifts are closely intertwined with a chronic, low-grade inflammatory state.

Diagnostic Criteria and Biomarkers in ALS

Because of the complexity of the not-fully understood ALS mechanisms, the multifactorial origin of the disease, and its phenotype heterogeneity, ALS diagnosis remains complicated and is mainly based on the exclusion of other pathologies. For the majority of patients, the diagnostic pathway is long and complex, due to the lack of reliable biomarkers and a high dependency on clinical evaluation. The most well-established criteria for ALS diagnosis are the Revised El Escorial, but their impact has been greater in clinical research than in clinical practice. As reported by Agosta and colleagues, the El Escorial criteria did not reduce the diagnostic delay (from 12 to 11 months), nor did they increase the accuracy of the diagnosis (which ranged from 37% to 30% of false-negative cases) (Agosta et al., 2015). The Awaji criteria only partially resolved the limitations of the Revised El Escorial, although they enhanced the overall sensitivity in ALS diagnosis up to 70% (Geevasinga et al., 2016).

Recently, the new Gold Coast criteria (GCc) were introduced to simplify and expedite the diagnosis of ALS, moving past the ambiguous categories of "possible", "probable" or "definite" ALS used by the previous criteria. As reviewed by Goutman et al., a GCc-based diagnosis requires progressive motor impairment, upper and lower motor neuron dysfunction in at least one body region (or lower motor neuron dysfunction in two body regions) and the exclusion of alternative diseases. Studies conducted in Australia, Europe, and China confirm that these parameters offer superior diagnostic sensitivity compared to the earlier El Escorial and Awaji criteria (Goutman et al., 2022). Despite the fact that the GCc represent a significant step forward, they present several limitations. In particular, the main one lies in the difficulty of objectively detecting upper motor neuron signs, which are often masked by muscle atrophy and weakness. This clinical ambiguity reduces diagnostic sensitivity, necessitating the integration of more objective techniques (Vucic et al., 2021).

To address the limitations in ALS diagnosis and staging, a wide expansion of methods and instruments has been recently observed. Functional and metabolic imaging are now essential for detecting early ALS alterations (van den Bos et al., 2019). Using magnetic resonance imaging (MRI) in combination with texture analysis software, selective neuronal vulnerability regions have been mapped in the corpus callosum of ALS patients (Münch et al., 2022).

Beyond imaging techniques, the diagnostic landscape of ALS is increasingly integrating also fluid biomarkers. In the cerebrospinal fluid, high levels of chitinases, namely CHIT-1 and CHI3L1 have emerged as stable indicators of neuroinflammation, remaining constant over time and effectively distinguishing ALS patients from healthy controls (Vu et al., 2020). Complementing this, non-invasive analysis of urinary samples revealed high levels of neopterin and $p75^{ECD}$ in ALS patients compared to healthy controls (HC). (Shepheard et al., 2022). Neurofilaments (NfL) have also emerged as pivotal fluid biomarkers, acting as downstream integrators of various pathological processes in ALS (Alshehri et al., 2024). Although levels are high in this disease, their dynamics are complex: their release into biofluids may not simply be proportional to axonal degradation but could reflect an adaptive response by motor neurons to conserve energy (Zucchi et al., 2018). In addition, phosphorylation of the neurofilaments heavy chain (pNfH) enhances its structural stability and solubility, directly modulating its axonal accumulation and subsequent detection within biofluids (Zecca et al., 2022). However, neurofilaments cannot be considered specific ALS biomarker, since increases in their concentrations is correlated with neuroinflammation and have been observed also in other neurodegenerative diseases like Alzheimer's disease and Multiple Sclerosis (Preische et al., 2019; Bjornevik et al., 2020).

Although significant insights have been gained, the current diagnostic landscape for ALS remains inadequate, underscoring an urgent and critical need to identify and validate novel biomarkers. While a growing array of innovative tools is emerging, most remain confined to research phases; bridging this gap is essential to transform these experimental methods into reliable clinical markers that can finally ensure a fast and precise diagnosis (Goutman et al.2022). In this context, monitoring the peripheral immune response represents a promising frontier, as disease progression has been closely linked to chronic neuroinflammation driven by a dysfunctional crosstalk between motor neurons and glial cells (Robberecht & Philips, 2011; Van Harten et al., 2021). Crucially, these neuroinflammatory processes alter the permeability of the blood-brain barrier (BBB) and the blood-spinal cord barrier (BSCB), which normally exert tight control over the influx and efflux of both cellular and molecular components. As reviewed by Pan & Nicolazzo (2022), the functionality of these barriers is typically compromised in ALS patients. This results in an increased leakiness of the BBB and BSCB, allowing plasma proteins and peripheral immune cells to easily extravasate and infiltrate the neuronal space.

ALS and Peripheric Immune System

In the last two decades, evidence of peripheral immune system involvement in ALS has grown significantly. While systemic alterations are now well-documented, contrasting results have been reported by different study. Moreover, their precise role in the pathogenic process remains to be fully elucidated; nonetheless, different peripheral cell populations may actively contribute to disease progression, either by participating in neurodegeneration or by exerting potential neuroprotective functions.

Lymphocytic infiltration in the spinal cord of a subset of patients was already observed during post-mortem analysis by Troost et al. in the late 80s (Troost et al., 1989). Subsequently, researchers sought to better elucidate the different behavior of the diverse immune populations. However, results differ significantly among studies. As reported by Murdock et al. (2017) the total leukocyte count in ALS patients showed higher values. According to the same study early-stage leukocytosis and neutrophilia are predictive of a more aggressive disease course, while decline in CD4 T-cell populations was positively correlated with a reduction in ALSFRS-R scores. Conversely, other studies evidenced increased levels of $CD4^+$ cells (Gustafson et al., 2017; Mantovani et al., 2009). Furthermore, a shift in T-cell subtypes towards pro-inflammatory T helper (Th)1 and Th17 cells has been observed by Jin et al. (2020) , which correlated with disease severity and progression. Interestingly, an animal model study by Chiu et al. (2008) confirmed a significant level of $CD4^+$ and $CD8^+$ T lymphocyte infiltration in the spinal cord of $SOD1^{G93A}$ mice. In the same model, ablation of these T-cells led to clinical worsening and reduced microglial activity. These findings support the hypothesis that certain T-cell responses may exert a neuroprotective effect. In contrast, the recruitment of $CD8^+$ T lymphocytes into the CNS has been documented during the symptomatic phase of this ALS mouse model (Coque et al., 2019). According to the same study, increased motoneuron survival was observed after $CD8^+$ T cells depletion, with MHC-I dependent interactions driving the neurotoxic effect. Furthermore, regulatory T cells (Treg), which are known to suppress the immune response, are likely to be involved in ALS pathogenesis. Dysfunctional Tregs have been observed in ALS patients, with reduced levels of these cells negatively correlating with disease progression (Mantovani et al., 2009; Rentzos et al., 2012; Henkel et al., 2013; Beers et al., 2017). The alteration of Treg cells and their neuroprotective effect have also been demonstrated by Banerjee et al. (2008) in $SOD1^{G93A}$ mouse models.

A major role for B cells in ALS pathogenesis was excluded by Noar and colleagues in 2009. They reached this conclusion after observing equal ALS development in both B-cell deficient $SOD\text{-}1^{G93A}$ mice and control $SOD\text{-}1^{G93A}$ mice (Naor et al., 2009). Although no apparent B-cell impairment has been reported in ALS patients, there is evidence that suggests an involvement of the humoral

component, especially immunoglobulins. Specifically, they observed a significant increase in circulating immune complexes (CICs) together with a higher concentration of IgG in patient serum; IgM levels were comparable between the two groups instead. Interestingly, while both high and low molecular weight CICs from controls were composed of IgG and IgM, high molecular weight CICs in ALS patients were predominantly composed of IgG (Saleh et al., 2009). IgG deposition within spinal motor neurons from ALS patients has previously been reported (Engelhardt & Appel, 1990). Moreover, there is evidence identifying several intracellular proteins involved in cytoskeletal architecture, RNA metabolism, and vesicular transport as targets of IgG autoantibodies in ALS patients (May et al., 2014). In addition, in animal models, disease-associated phenotypes have been induced through long-term serum administration, with increased animal weakness and significant loss of motor neurons observed (Obál et al., 2019). While the primary autoimmune etiology for ALS remains unproven, these findings strongly suggest an autoimmune-like involvement in promoting neurodegeneration. As discussed by Obál and colleagues, the production of motor neuron-targeted IgG could stem from two potential scenarios: a specific immune sensitization to neuronal proteins that accelerates cell death, or a secondary immune response triggered by the release of intracellular debris from independently degenerating neurons. In both cases, this humoral response likely acts as a detrimental feedback loop, where circulating autoantibodies and local IgG deposition can collectively aggravate neuroinflammation and exacerbate motor neuron damage.

Furthermore, monocyte infiltration has been observed in the spinal cord of patients (Zondler et al., 2016). Zondler and colleagues also reported a different distribution of monocytes between patients and controls. In particular, while in the healthy spinal cord the majority of $CD169^+$ monocyte-derived cells were located perivascularly, in ALS patients they mainly localized deeper in the damaged tissue. Moreover, ALS appears to be linked to changes in circulating monocytes' functional and expression profiles. A switch toward a pro-inflammatory state has been observed by Zhao et al. (2017) after RNA sequencing of isolated peripheral monocytes. To support this finding, an increased expression of pro-inflammatory cytokines has been observed after macrophage differentiation from ALS circulating monocytes compared to healthy control macrophages (Du et al., 2020). Besides that, a possible association between disease progression and different prevalence rate of monocytic subtypes has been proposed. Zhang et al. (2005) observed a correlation between the number of $CD14^+$ $HLA\text{-}DR^+$ activated macrophages and ALSFRS-R scores, where higher numbers were associated with faster disease progression. However, conflicting evidence exists related to the abundance of monocytes between ALS patients and controls. While some studies reported an increased monocytic fraction in the presence of the disease (Mantovani et al., 2009), other authors claimed no major differences were detected (Zhang et al., 2005).

Recently, granulocyte alterations have been observed in the context of ALS pathology, with patients showing higher granulocyte levels compared to HC (Gustafson et al., 2017). According to the findings reported by Murdock et al. (2016), even though the total leukocyte count remained comparable to HC, ALS patients showed higher neutrophil percentages. Moreover, increased infiltration and activation of neutrophils and mast cells have been observed in the quadriceps muscles from ALS patients during autopsy analysis. In particular, the cytotoxic effect of neutrophil activation is underlined by the increased formation of neutrophil extracellular traps in association with motor endplates, suggesting a direct activity against neuromuscular junction elements (Trias et al., 2018).

NK cells contribute to ALS pathology, with evidence of NK alterations identified in both human patients and animal models. Infiltration of this immune population has been noted in the motor cortex and in the spinal cord of ALS patients and in $SOD1^{G93A}$ mice after post-mortem tissue analysis (Garofalo et al., 2020). In the same animal model, Finkelstein and colleagues also observed increased NK levels in the spleen and liver (Finkelstein et al., 2011). In a study regarding human ALS patients, increased levels of NK cells were also reported after the analysis of immune cells isolated from peripheral blood (Rentzos et al., 2012). Although the mechanisms remain partially unknown, the negative contribution of this cellular population to ALS pathology has been clearly stated. A dual role for NK cells has been reported in $SOD1^{G93A}$ mice: a direct neurotoxic effect on motoneuron, alongside an indirect effect driven by cytokine release. In particular, interferon (IFN)-γ expressed by NK cells impaired Forkhead box P3 ($FOXP3^{+)}$ Treg cell infiltration into the spinal cord and led to microglia activation toward a pro-inflammatory phenotype (Garofalo et al., 2020). Interestingly, NK cells apparently contribute to ALS progression in a sex-specific manner. This hypothesis is supported by results obtained after depletion of this cellular population in ALS models, which extended the survival time only in female mice (Murdock et al., 2021). According to the same study, increased expression of homing and cytotoxicity surface markers has been observed in ALS patients. Moreover, this was also associated with the ALSFRS-R score in an age- and sex-specific manner (Murdock et al., 2021).

Alterations in BBB/BSCB integrity together with changes in peripheral immune cell populations support the existence of a systemic component of the disease, providing a strong rationale for the identification of ALS-associated biomarkers in peripheral blood. The discovery of such biomarkers would represent a significant step forward in ALS diagnosis, facilitating earlier and more accurate disease detection as well as improved prognostic stratification of patients.

Objective of the Thesis

The objectives of this project are structured in two sequential steps. The first aim is to identify novel cellular biomarkers associated with ALS through high-dimensional multiparametric flow cytometry. Using an unsupervised analysis of the peripheral blood immune landscape, this discovery phase seeks to uncover candidate immune signatures with potential diagnostic and prognostic relevance.

Based on these initial findings, the second aim is to develop and validate a dedicated flow cytometry panel for in-depth characterization of the most relevant leukocyte subsets identified in the discovery phase. This targeted panel will be optimized on healthy donor samples through systematic fluorochrome selection and methodological refinement, establishing a robust framework for subsequent functional and translational studies of these immune populations in the systemic inflammatory context of ALS.

Material and Methods

Phase One: Immunophenotyping

Data Collection from the Cohort's Patients

The study was conducted at the Expert ALS Center (CRESLA) of the 'Maggiore della Carità' University Hospital in Novara, between January 2020 and October 2021. The cohort consisted of twenty-four patients with a diagnosis of definite Amyotrophic Lateral Sclerosis (ALS) and fifteen age-matched healthy controls (HCs). The mean age was 59 years for the ALS group and 61 years for the HCs. At baseline, comprehensive demographic and clinical data were recorded, including age at symptom onset, clinical phenotype, and disease severity as assessed by the ALS Functional Rating Scale-Revised (ALSFRS-R). Additional parameters included Forced Vital Capacity (FVC%, expressed as a percentage of the predicted value), Body Mass Index (BMI), comorbidities, and cognitive status according to the Strong criteria (Strong et al., 2017). The presence of known genetic mutations was also documented. Furthermore, clinical data were collected longitudinally throughout the disease course to monitor progression. Survival time was defined as the interval from symptom onset to death or tracheostomy. The HCs, primarily spouses or acquaintances of the patients, were selected to ensure age-matching and the absence of neurological disorders.

The study received approval form the Ethics Committee of the "Maggiore della Carità" University Hospital (CE No. 184/20). All enrolled subjects provided written informed consent for their participation in the study and for the collection of blood samples.

Immunofluorescence Staining and Acquisition for Immunophenotyping

Peripheral blood samples were collected into K2EDTA tubes (BD Biosciences). Two hundred µL of unmanipulated whole blood was incubated with 19 different fluorochrome-conjugated antibodies in the same tube, all titrated to their optimal concentrations, in Brilliant Stain Buffer (BD Biosciences). The antibody panel included CD183 (CXCR3) in APC, CD3 in BUV496, CD123 in PECY5, CD196 (CCR6) in BV480, CD8 in BUV805, CD25 in APCR700, CD197 (CCR7) in BV711, CD20 in BV750, CD11c in BUV661, CD24 in BB515, CD38 in BV650, CD16 in BB780, CD19 in BUV615, CD45 in BUV395, CD45RO in PE-Cy7, CD194 in PE-CF594, CD4 in BUV737, CD45RA in BUV563, and HLA-DR in BV605. The incubation lasted 20 minutes and underwent at RT in dark conditions.

To remove red blood cells after monoclonal antibody staining, PharmLyse™ lysing solution (BD Biosciences) was used. Each sample received 2 ml of lysing solution and underwent lysis for 20 minutes at RT. Samples were then washed twice with 2 ml of 1X phosphate buffered saline (PBS) containing 2 mM EDTA. After each 1x PBS 2mM EDTA addition, cell were centrifugated (1500 rpm; 5 minutes) and supernatant has been discarded. Subsequently, all samples were resuspended in 200 µl of 1X PBS 2mM EDTA solution and analyzed using the FACSymphony™ A5 flow cytometer.

Data Pre-Processing and Gating Strategy Prior Unsupervised Analysis

To ensure high data quality for downstream unsupervised analysis, a rigorous pre-processing cleaning procedure was performed on all samples. Initially, cell doublets and aggregates were excluded using an FSC-H vs. FSC-A plot (Figure 2A). Since single cells maintain a linear proportionality between signal height and area, events deviating from this diagonal were discarded to prevent the algorithm from misinterpreting aggregates as hybrid or novel cell populations. Morphological selection was then performed using an SSC-A vs. FSC-A plot (Figure 2B) to identify the lympho-monocyte region. This step excluded cellular debris, characterized by low FSC-A, and granulocytes, characterized by high internal complexity (high SSC-A). To ensure the purity of the analyzed fraction, a pan-leukocyte gate was applied using the CD45 marker in combination with SSC-A (Figure 2C). This further differentiates white blood cells from CD45-negative contaminants, such as residual red blood cells, platelets, and debris. Finally, the fluorescence signal stability of the gated $CD45^+$ population was monitored over Time (Figure 2D). This final quality control step was performed to ensure that the events were not affected by fluidic fluctuations, electronic noise, or laser instability during the entire duration of the sample acquisition.

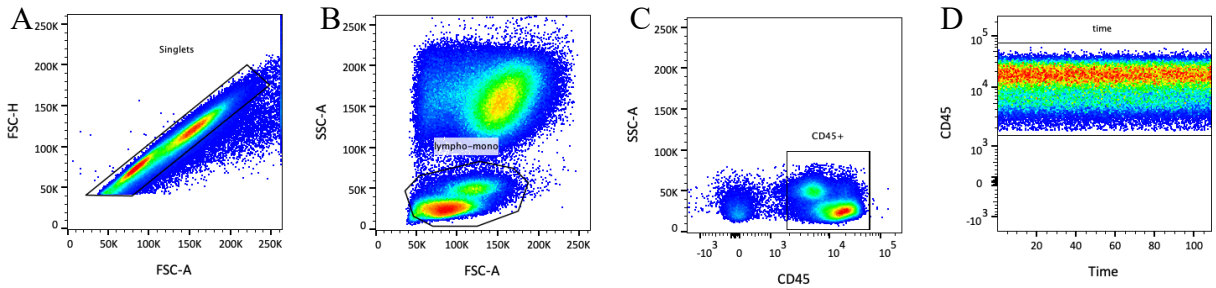

Figure 2: Gating strategy adopted for cleaning samples. **A.** Singlets identification (FSC-H vs FSC-A). **B.** Morphologic gate for lymphocytes and monocytes identification (SSC-A vs FSC-A. **C.** CD45 positive cells' gating (SSC-A vs CD45). **D.** Time gate of CD45 positive cells to exclude flow issues during the acquisition.

Unsupervised Analysis of Flow Cytometry Data

For the unsupervised analysis, a down-sampling procedure was performed to randomly select 10^4 CD45+ events per sample. This step was crucial to ensure an equal statistical contribution from each patient and to maintain computational efficiency during data processing. The resulting file were concatenated into a single dataset and analyzed using the OMIQ data analysis software (OMIQ, Inc., Santa Clara, CA, USA).

To visualize the high-dimensional immune landscape in a 2D space, the PaCMAP (Pairwise Controlled Manifold Approximation) algorithm was applied. Automated clustering was then performed using the FlowSOM algorithm. A self-organizing map was generated and subsequently subjected to meta-clustering with a predefined value of $k = 30$. This number of clusters was selected to provide sufficient resolution for identifying rare sub-populations (such as basophils and specific dendritic cell subsets) while avoiding over-segmentation of major lineage groups.

Finally, the resulting meta-clusters were backgated and visualized on traditional dot plots to validate their phenotype. This manual confirmation ensured that the automated clusters corresponded to consistent biological populations, which were then named according to their specific marker expression profiles.

Statistical Analysis

Statistical processing of flow cytometry data was performed using FlowJo, for manual gating and validation, and OMIQ software, for high-dimensional unsupervised analysis. All downstream statistical evaluations and data visualizations were conducted using GraphPad Prism (version 10, Boston, MA, USA) and R-based computational tools.

To evaluate differences in immune cell subsets between ALS patients and Healthy Controls, the non-parametric Mann-Whitney U-test was employed. For clinical comparisons an unpaired Student's T-test was used. Throughout the study, statistical significance was defined as a p-value ≤ 0.05.

Phase Two: New Panel for Basophils

Marker Selection for Specific Panel Constitution

In the previous immunophenotyping analysis, the panel was designed to broadly characterize multiple immune cell populations within the cohort. However, basophils were not extensively investigated, as their identification relied on a limited set of markers, namely CD123 in combination with HLA-DR negativity. Although this strategy is commonly used for basophil detection, the restricted phenotypic characterization did not allow for an in-depth evaluation of basophil heterogeneity or activation states. The selection of markers was based on a comprehensive review of current literature, prioritizing antigens that allow for the identification and functional assessment of this rare cell population. To ensure high purity, a 'Dump Channel' strategy was implemented; this included antibodies against CD3, CD14, CD16, CD19, and CD56 to exclude T cells, monocytes, B cells, and NK cells. Basophils are characterized by strong expression of CD38 and CD11c, while they generally display intermediate positivity for CD45 and CD11b. Another established strategy to identify basophils is the use of CD123 in combination with HLA-DR (negative selection). Alternatively, FcεRI can be employed in combination with CD123, CD203c, or IgE. Furthermore, CD193 can be used alongside CD3 to distinguish basophils from Th2 cells. CD294 is also valuable for discriminating between basophils and eosinophils; indeed, while both populations are positive for this marker, they can be distinguished by their different SSC (Side Scatter) signals, which reflect their distinct internal complexity.

Moreover, the panel incorporated several markers to evaluate cellular activation and degranulation dynamics. CD63 and CD203c were selected as primary indicators of activation. Additionally, markers such as CD13, CD107a, CD107b, CD69, and CD164 were included to capture a broad spectrum of the basophil activation profile. Finally, CD244 was added to investigate its potential role in immune modulation, given its reported association with disease progression in autoimmune and inflammatory contexts.

A comprehensive summary of the selected markers, along with the rationale for their use and corresponding bibliographic references, is provided in the Table 1 in the next page.

Category	Marker	Presence on Basophils	Rationale of the choice	References
Lineage Exclusion	CD3, CD14, CD16, CD19, CD56	Negative	Dump channel for exclusion of T, B, NK cells, monocytes, and neutrophils.	-
Identification	CD123	High Positive	Primary marker for basophil identification.	Sonder et al., 2023
	HLA-DR	Negative	Combined with CD123 to distinguish basophils from DCs.	Sonder et al., 2023
	FcεRI / IgE	Positive	High-affinity IgE receptor/surface IgE for basophils identification.	Sonder et al., 2023
	CD11c / CD38	Positive	Supporting markers for lineage confirmation.	-
	CD193 (CCR3)	Positive	Differentiation from Th2 cells (when combined with CD3).	Sonder et al., 2023
Activation	CD63 / CD203c	Inducible/High	Primary markers for degranulation and activation monitoring.	Kim et al., 2016
	CD13, CD69, CD107a, CD107b, CD164	Inducible	Broad-spectrum assessment of activation dynamics.	Hennersdorf et al., 2005
Modulation	CD244	Positive	Modulated in basophils subsets	Berger et al., 2021 ; Sun et al., 2021 ; Munitz et al., 2005

Table 1: Selection and rationale of the markers included in the basophil-focused antibody panel. The selected markers are categorized based on their specific role in the immunophenotyping strategy. The Lineage Exclusion group defines the "Dump Channel" used to eliminate non-target populations. The Identification category includes primary and supporting markers for the definitive isolation of basophils and their discrimination from phenotypically similar subsets (e.g., pDCs, eosinophils, and Th2 cells). Activation and Modulation markers were selected to monitor degranulation dynamics and immune-modulatory profiles, respectively. Expected expression patterns on basophils and supporting bibliographic references are provided for each antigen.

Antibody Titration Procedure

Each antibody-fluorochrome conjugate has been individually titrated to optimize its concentration, in order to achieve the better acquisition performance achievable. Starting with the manufacturer's recommended concentration, a series of four two-fold serial dilutions (1X; 0,5X 0,25X; 0,125X) were prepared in Pharmigen™ Stain Buffer (BD Bioscences). Twenty µL of Brilliant Stain Buffer (BD Bioscences) were added to each dilution. Subsequently, peripheral whole blood collected from healthy volunteer has been lysate to isolate leukocytes. Lysing solution has been prepared by diluting PharmLyse™ lysing solution (BD Biosciences) 1:10 in deionized water (mqH_2O). Three and half mL of peripheral whole blood have been added to 45 mL of the lysing solution and incubated on rocking platform for 15 minutes at room temperature. The resulting cell suspension was centrifugated at 423 g for 5 minutes (this setting has been maintained for all subsequent steps) and washed twice with 50 mL of staining buffer (1X PBS supplemented with 2mM EDTA and 1% FBS). After each centrifugation, the supernatant was discarded and cell pellet was gently resuspended by vortexing.

Two million of cells have been incubated with a single antibody dilution for 20 minutes at RT in dark conditions. Samples were then washed with 2 mL of staining buffer (1X PBS supplemented with 2mM EDTA + 1% FBS) and resuspended in 300 µL of the same media for the acquisition process. (FACSymphony™ A5 flow cytometer).

Immunofluorescence Staining Protocol for Basophils Identification

Peripheral blood samples were collected in K2EDTA tubes and lysed as described previously. Following the second wash, cells have been resuspended in 1 mL of staining buffer and quantified. For each immunofluorescence staining, 2 x 10^6 cells were used. Cells were transferred into a flow cytometry tube and washed with 2 mL of protein-free PBS (1X PBS supplemented only with 2 mM EDTA) to remove residual FBS, which could interfere with the subsequent viability staining. The cell pellet was then incubated with 500 uL of Fixable Viability Stain 780 (BD Biosciences), diluted 1:1000 in protein-free PBS, for 20 minutes at 4°C. After incubation, cells were washed with 2 mL of staining buffer; the inclusion of 1% FBS in this step ensured the neutralization of any unbound viability dye.

The antibody mix was then prepared. To prevent non-specific interaction between fluorochromes and to reduce spreading error, 20 µL of Brilian Stain Buffer (BD Biosciences) per sample were added as first component of the antibody mix. Cells were incubated with the antibodies for 20 minutes at room temperature in dark conditions. Finally, samples were washed with 2 mL of staining buffer and resuspended in 300 µL of staining buffer for flow cytometry acquisition (FACSymphony™ A5 flow cytometer).

Results

Immune Signature of ALS Patients

Characterization of the Cohort

The study cohort consisted of 24 ALS patients (13 males and 11 females), with a mean age at onset of 58 years and an average diagnostic delay of 11 months. Regarding clinical history, significant comorbidities were identified in two patients, specifically diabetes and hypothyroidism. In another instance, while diabetes was clinically excluded, additional endocrine data remained unavailable. Genetic screening revealed that the majority of the cohort consisted of sporadic cases (n=18), whereas the remaining six patients carried known ALS-related mutations, specifically in C9orf72 (n=5) and KIF5A (n=1).

In terms of clinical presentation, the majority of the cohort (71%) exhibited spinal onset, while seven patients presented with bulbar symptoms. Phenotypic classification showed that 12 patients had classic ALS; the remaining cases were characterized by bulbar (n=7), flail arm (n=1), or upper motor neuron-dominant (n=4) forms. Cognitive function was preserved in the majority of the group (79%), although five patients exhibited ALS-related cognitive impairment. To evaluate disease dynamics, patients were stratified by their ALS Functional Rating Scale-Revised (ALSFRS-R) progression rate: 10 were classified as slow progressors (SPs) and 14 as fast progressors (FPs), based on a standard cutoff of 0.8 points/month. At baseline, the cohort showed a median BMI of 23.2, an FVC% of 89%, and a median ALSFRS-R score of 41.5.

Immunophenotypic Comparation Between ALS Patients and HC

Flow cytometry data were pre-processed and cleaned following the procedures detailed in the Materials and Methods section. To identify high-dimensional relationships and uncover novel cell populations, the cleaned data underwent unsupervised computational analysis. Based on the differential expression of markers, 21 distinct cell clusters were identified; these have been then visualized in a two-dimensional space using the PaCMAP algorithm. This method has been chosen because it ensures the preservation of the global and local landscape topology. As shown in Figure 3, the algorithm was able to precisely resolve the different leukocyte lineages, from T and B cells compartments to myeloid subpopulations that appear as phenotypically distinct and well-separated aggregates.

Subsequently, a heatmap was generated (Figure 4) to analyze the expression profile of phenotypic markers across the identified clusters. This representation allows for the validation of the immunological identity of each population based on differential protein expression, providing biological confirmation of the unsupervised clustering. The expression profile faithfully reflects the organization of the major leukocyte lineages: T cells compartments are clearly defined by CD3 positivity and the mutual exclusion of CD4 and CD8, while B cells are identified by the co-expression of CD19 and CD20. NK populations show expression of CD16 in absence of CD3. Similarly, the myeloid compartment shows accurate segregation of CD14 positive monocytes. Basophils also emerged as a distinct phenotypic entity, uniquely characterized by high expression of the CD123 in absence of HLA-DR expression.

Comparing the abundance of the different immune population within patients and healthy controls (HC) revealed that basophil levels were significantly elevated in ALS patients. This finding was further supported by volcano plot analysis (Figure 5), which emphasized the statistical significance and fold-change relevance of this population in the disease context.

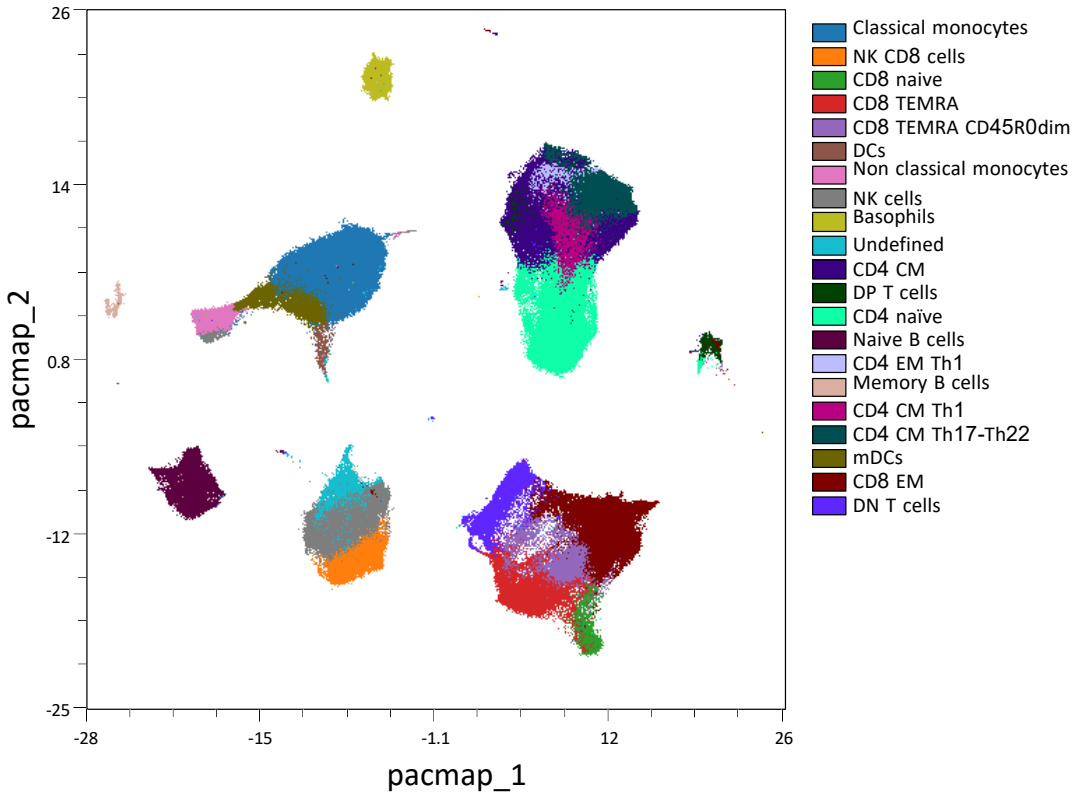

Figure 3: Two-dimensional visualization of cell clusters using the PaCMAP algorithm. Projection of pre-processed flow cytometry data where 21 distinct clusters have been identified based on differential marker expression. The spatial arrangement along the *pacmap_1* and *pacmap_2* axes demonstrates the phenotypic resolution of various leukocyte lineages. Each dot represents a single cell, color-coded according to its assigned cluster via unsupervised computational analysis.

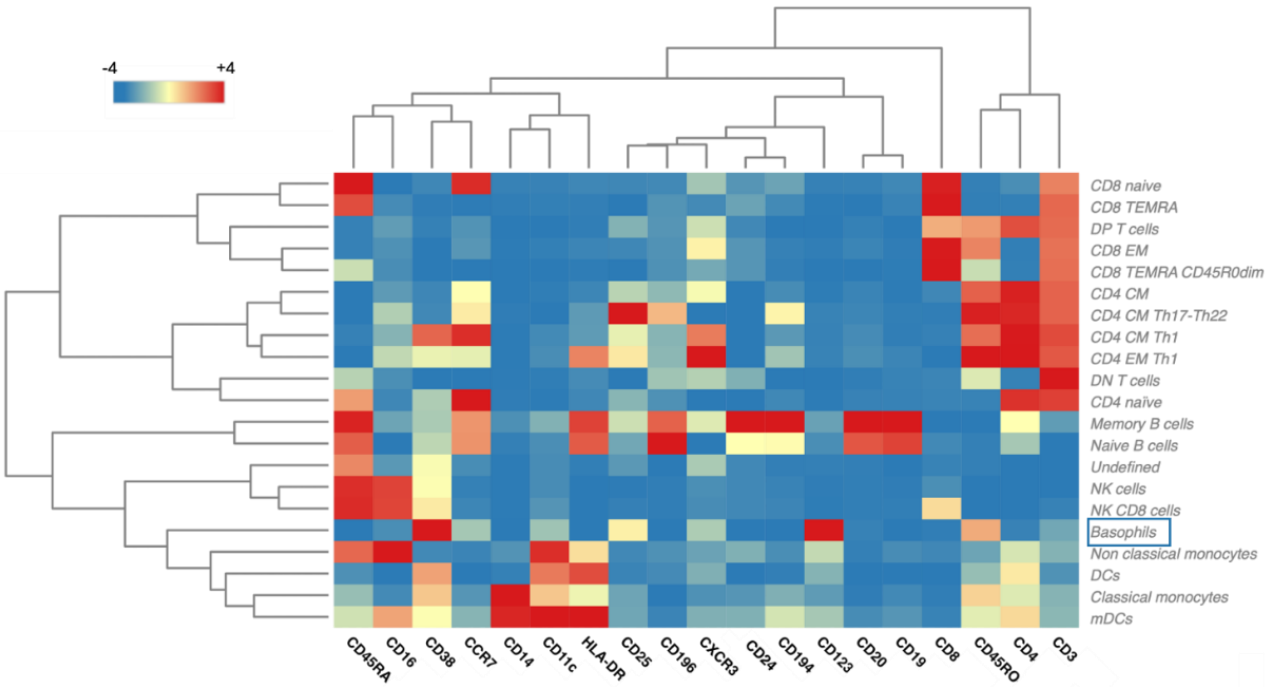

Figure 4: Hierarchical clustering and heatmap of phenotypic marker expression. Heatmap showing the differential expression profiles of protein markers across the identified leukocyte clusters. The dendrogram represents the hierarchical relationship between clusters based on marker expression levels. The color scale indicates the relative expression levels of markers, ranging from blue (low expression, -4) to red (high expression, +4). The blue box highlights the specific phenotypic profile of the basophil cluster.

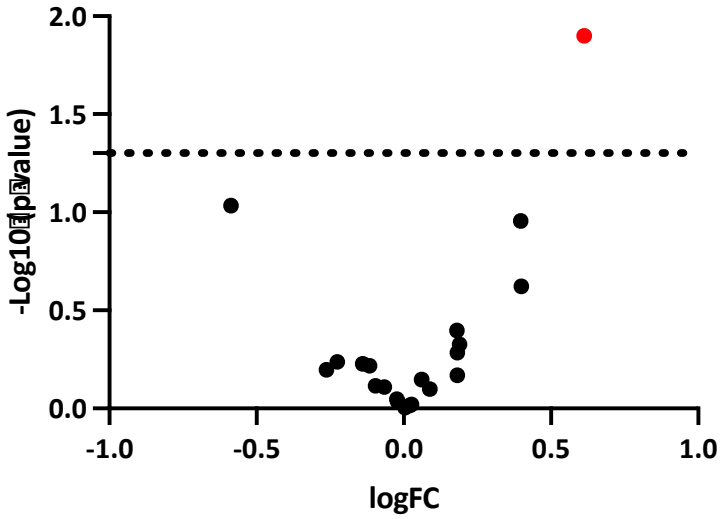

Figure 5: Volcano plot showing the difference in abundance of immune cell populations between ALS patients and HC. The plot illustrates the relationship between statistical significance ($-log_{10}\ p\ value$) and the magnitude of change ($\log FC$) . The dotted horizontal line represents the threshold of p = 0.05 ($-log_{10}\ 0.05\ \approx 1.3$) for statistical significance. Positive $\log FC$ (right side of the plot) indicates an increase in ALS patients, while a negative $\log FC$ (left side) would indicate a decrease. The red dot identifies the basophil population, which is significantly elevated in ALS patients compared to HCs, demonstrating both high statistical significance and a positive fold-change. Mann-Whitney test T test were used.

In order to ensure that the populations identified through unsupervised clustering reflected biologically meaningful and not purely algorithm-driven structures, a validation step based on traditional flow cytometry principles was required. While high-dimensional clustering approaches enable an unbiased exploration of cellular heterogeneity, they may occasionally generate partitions that are difficult to directly interpret in conventional cytometric terms. For this reason, a back-gating approach was implemented to project the identified clusters onto classical two-dimensional marker spaces. This step allows direct assessment of their spatial distribution within established immunophenotypic frameworks. In particular, it provides a critical bridge between data-driven classification and standard gating strategies. Thus, a retrospective back-gating strategy specifically targeting basophils was performed. This manual validation confirmed the significant expansion of basophils in the ALS cohort, demonstrating high consistency between unsupervised clustering and traditional gating (Figure 6).

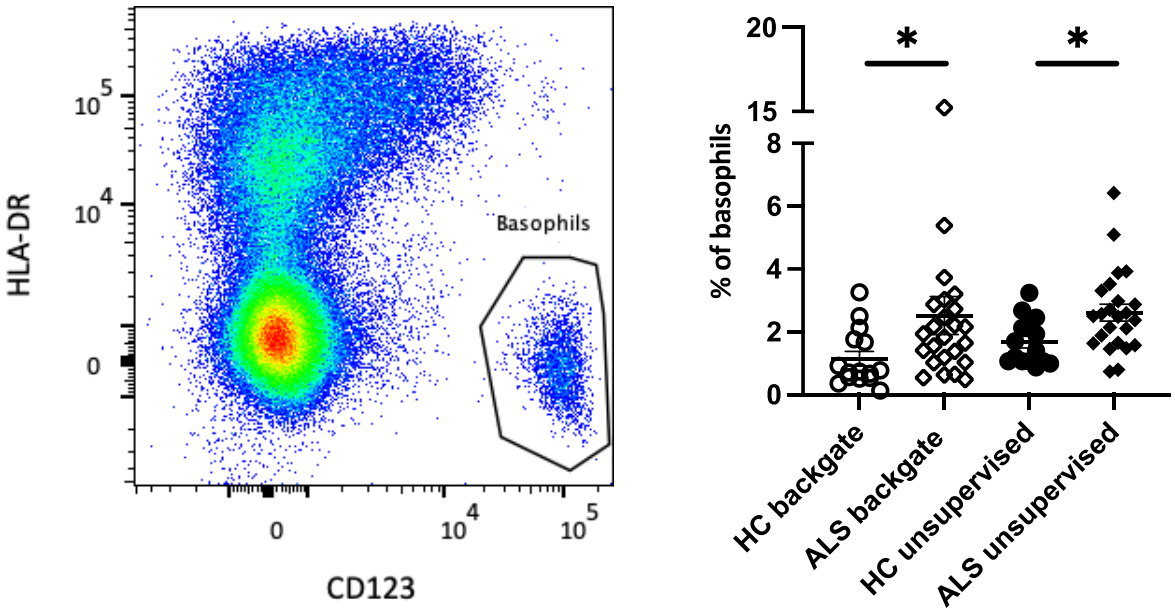

Figure 6: Validation of basophil expansion via manual back-gating. (*On the left*) Representative dot plot showing the gating strategy used to identify the basophil population, defined by high CD123 expression and the absence of HLA-DR. (*On the right*) Comparison of basophil frequencies between healthy controls (HC) and ALS patients. The analysis demonstrates a significant increase in the percentage of basophils in the ALS cohort, with high consistency between the results obtained through manual back-gating and those from the unsupervised computational analysis. Mann-Whitney U test was used. * $p<0.05$.

Immune Signature Differences Between Slow and Fast Progression in ALS Patients

We subsequently investigated potential associations between the 21 identified clusters and clinical parameters, including phenotype, disease progression, and cognitive status. While genetic background and cognitive impairment showed no significant correlation with cluster distribution, a robust association emerged regarding disease progression. Specifically, slow progressors (SPs) exhibited significantly higher levels of two myeloid subtypes: basophils (Figure 7A) and classical monocytes (Figure 7B). Conversely, a reduction in CD4+ naïve T cells was observed in the same patient group (Figure 7C), suggesting the presence of divergent immune signatures distinguishing SPs from fast progressors (FPs).

To ensure these immunological differences were not influenced by baseline clinical disparities, we compared SPs and FPs at the time of diagnosis. The two groups were comparable across all primary variables, including sex, phenotype, cognitive status, ALSFRS-R score, BMI, and FVC% ($p>0.05$).

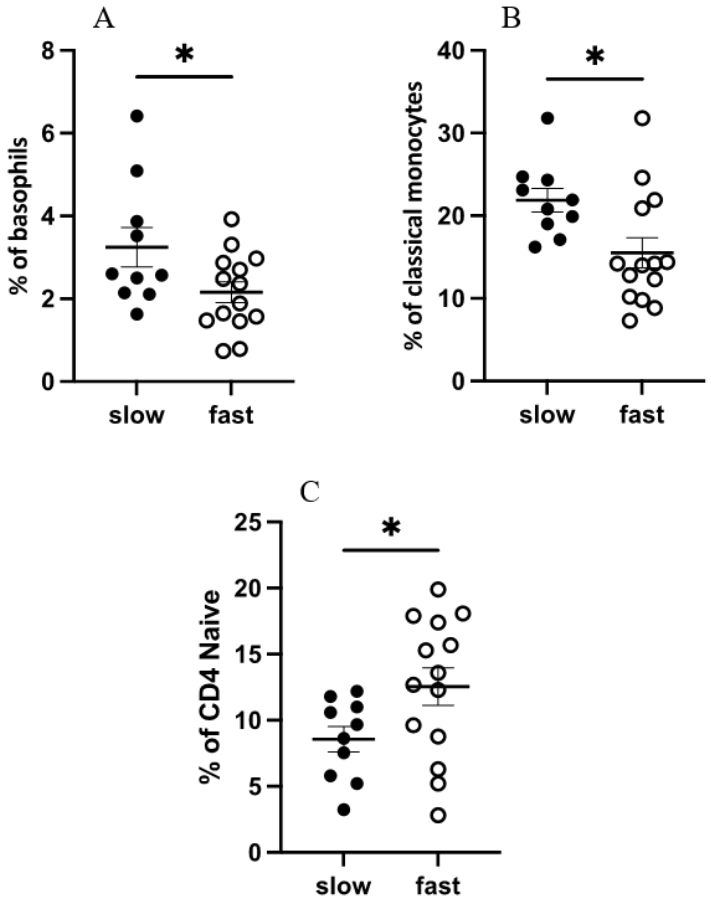

Figure 7: Correlation between leukocyte cluster frequencies and ALS disease progression. Scatter dot plots comparing the percentages of specific cell populations between SP (slow) and FP (fast). **(A)** Basophil levels are significantly higher in the slow progressor group compared to fast progressors. **(B)** Similarly, classical monocytes exhibit a significant increase in slow progressors. **(C)** In contrast, the percentage of CD4+ naïve T cells is significantly reduced in slow progressors compared to fast progressors. Horizontal lines represent the mean with error bars. Mann-Whitney test was used; * $p<0.05$.

Panel Set Up for Basophils Subpopulation Identification

Antibody Titration and Preliminary Panel Setup

Because the most significant alterations in the immune signature of ALS were identified within the basophil compartment, a dedicated antibody panel was subsequently developed to further characterize this cellular population. Moreover, the panel has been designed also for T and B cells identification, and for distinction of different monocytes subpopulation (Classical, Non-classical and Intermediate monocytes respectively). Markers have been selected as described in the Material and Methods section.

Prior to final panel constitution, each marker has been individually titrated to optimize its visualization. This passage is fundamental during a panel setup; an insufficient antibody concentration precludes the effective discrimination between positive signals and background noise, whereas an excessive concentration increases the risk of signal saturation and non-specific binding. Individual dilutions of each antibody have been prepared as described in the Materials and Methods section. The stain index (SI) was then calculated for each dilution (Table 3) and an antibody titration multigraph (Figure 8) was generated to visually evaluate acquisition performance across the dilution range. The optimal concentration was determined by maximizing the SI and ensuring the clearest separation between positive and negative populations.

V/test	MFI (+)	MFI (-)	rSD (-)	SI
5 µL	1899	86.1	74.2	12.21630728
2.5 µL	1445	44.9	57.8	12.1115917
1.25 µL	1136	24.4	46.2	12.03030303
0.625 µL	767	10.3	34	11.2794118

Table 3: Quantitative parameters for the evaluation of staining efficiency across a range of FcεRI volumes. Data include Median Fluorescence Intensity (MFI) for positive and negative populations, robust Standard Deviation (rSD), and the calculated SI. MFI and rSD values were automatically generated by FACSDiva™ software (BD Biosciences). The green row indicates the antibody concentration selected for the final staining protocol. $SI = \frac{[MFI(+)] - [MFI(-)]}{2 * [rSD(-)]}$

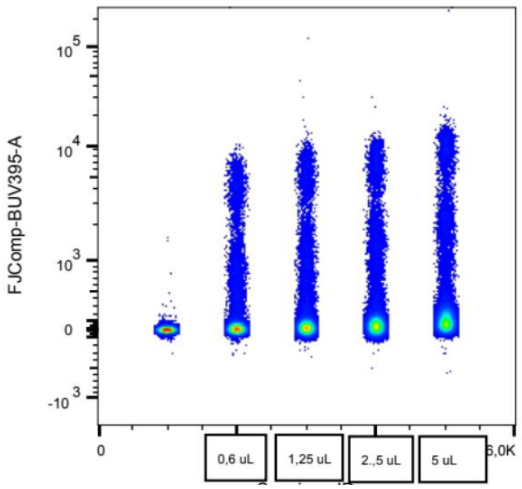

Figure 8: Visual assessment of signal resolution for the BUV395-A channel (FcεRI). The graph displays the different ability to discriminate positive and negative populations across the dilution range described in Table 2, supporting the selection of 5 µL as the optimal volume for the final panel.

Following the optimization of individual antibody concentrations, a preliminary multi-color panel was created. This initial configuration combined lineage markers for broad population identification, specifically CD3; CD11b; CD11c; CD14; CD16; CD19; CD45; CD56; and HLA-DR, with a specialized subset designed for basophil characterization and activation monitoring, including CD123; FcεRI; IgE; CD63; CD69; CD193; and CD203c. To complete the functional profile of the panel, additional markers were integrated, namely CD13; CD38; CD107a; CD107b; CD164; and CD244.

Evaluation of Spectral Overlap and Panel Refinement

The optimized panel, summarized in Table 4, was standardized for the staining of 2×10^6 cells per sample, providing a robust tool for the simultaneous characterization of leukocyte lineages and the deep phenotyping of the basophil compartment.

Antibody	Fluorochrome	µL per sample
L/D (Fixable Viability Stain 780)	APC-Cy7-A	500*
Brilliant Stain Buffer	-	20
CD14	AF647	20
CD164	RB744	20
CD3	BUV496	10
CD107b	BV786	10
CD11c	PerCP-CY5-5	10
CD107a	RB780	7
CD123	RY610	5
CD244	BV421	5
CD69	RB613	5
FcεRI	BUV395	5
CD38	BV510	2,5
CD11b	AF488	2,5
IgE	BUV563	2,5
CD13	BUV661	1,25
CD16	BUV615	1,25
CD19	BV605	1,25
CD193	BV711	1,25
CD203c	R718	1,25
CD56	PE-Cy7	1,25
CD63	BV650	1,25
CD45	BUV737	0,625
HLA-DR	BUV805	0,625

Table 4: Final optimized panel for monocytes and basophil phenotyping. The table summarizes the definitive antibody and reagent configuration. For each target, the associated fluorochrome and the optimized volume per test are reported. The configuration reflects the final refinement steps, including the exclusion of the CD294 marker and the inclusion of Brilliant Stain Buffer (BD Bioscences) to prevent polymer-dye interactions. **(*)** The Fixable Viability Stain 780 was used in a separate incubation step prior to the addition of the antibody mix, as indicated in the section "Immunofluorescence Staining Protocol for Basophils Identification".

HD have been fundamental also for the validation of the gating strategy (illustrated in detail in Figure 9). By employing this specific antibody panel, we successfully identified the following major immune cell populations: T cells, B cells, NK cells, monocytes, and basophils. Monocytes were further characterized into three distinct subsets based on their CD14 and CD16 expression, respectively Classical Monocytes ($CD14^+$ $CD16^-$), Intermediate Monocytes ($CD14^+$ $CD16^+$) and Non-classical Monocytes ($CD14^-$ $CD16^+$). Regarding basophils, the identification approach was based on a four-round gating strategy (specifically HLA-DR^-/Fc$\epsilon$$RI^+$, HLA-$DR^-$/$CD123^+$, HLA-$DR^-$/$IgE^+$, and Fc$\epsilon$$RI^+$/$IgE^+$ respectively) in order to achieve the highest possible purity for subsequent analysis. Consequently, based on their functional characterization, we were able to identify seven basophil subsets (Figure 10), respectively $CD63^+$ basophils (Figure 10A), $CD69^+$ basophils (Figure 10A), $CD107b^+$ basophils (Figure 10B), and $CD203c^+$ basophils (Figure 10C). Interestingly, the different level of CD164 expression allowed for the subclassification within three different subsets (Figure 10D), namely $CD164^{neg}$ basophils, $CD164^{med}$ basophils, and $CD164^{high}$ basophils. It is worth noting that these seven functional subsets are not mutually exclusive, as individual basophils can co-express multiple activation markers depending on their functional state.

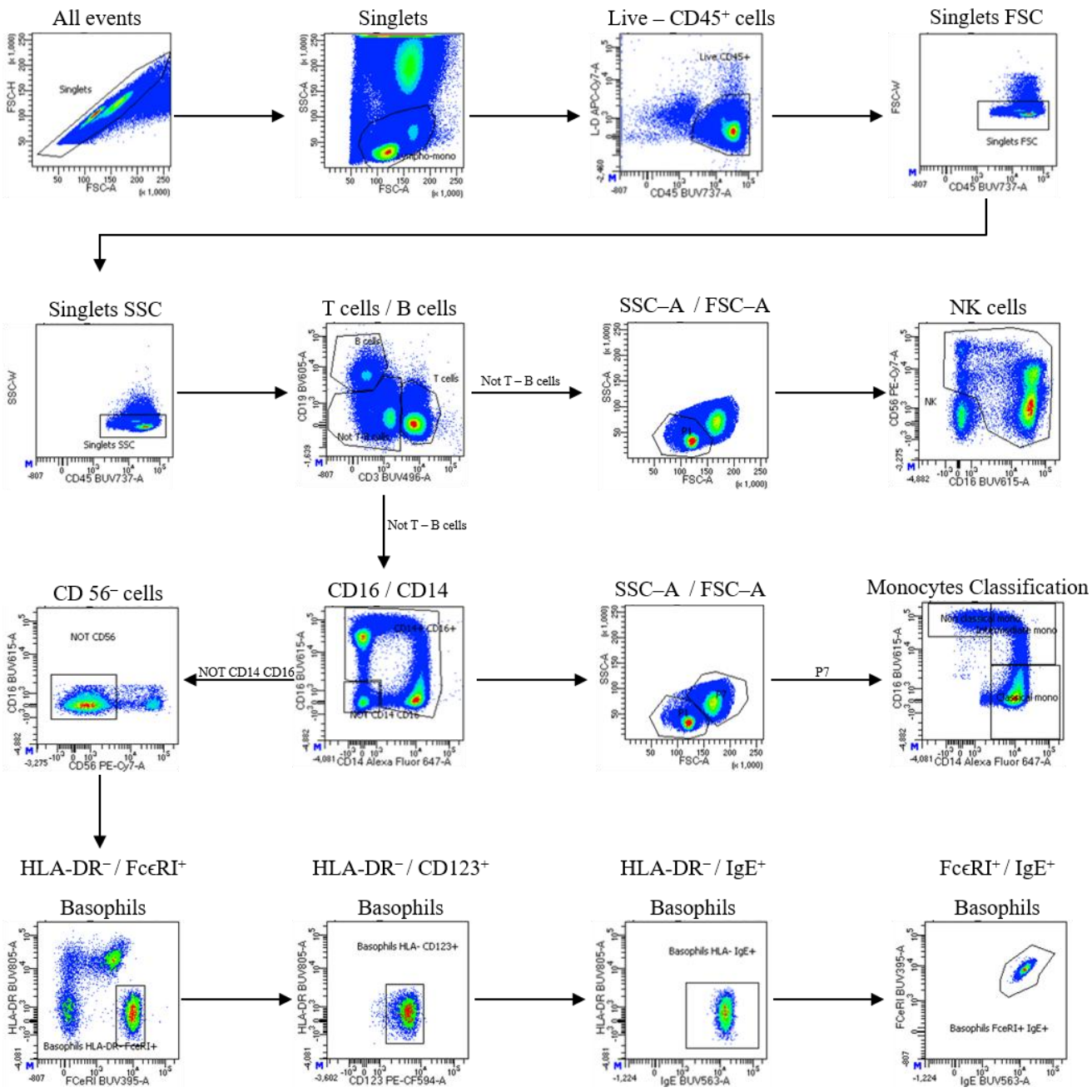

Figure 9: Hierarchical gating strategy for the identification of major leukocyte populations including NK cells, monocytes, and basophils. Representative flow cytometry plots illustrating the multi-step gating strategy. The arrows indicate the hierarchical progression of the gating logic. The analysis begins with an initial doublet exclusion (Singlets FSC-H/A) followed by a morphological selection of the lympho-monocyte population. Within this gate, viable leukocytes are identified as Live-CD45+ events. To ensure maximum data stringency, two additional consecutive doublet exclusion steps are performed using side scatter (Singlets SSC-W/CD45) and forward scatter (Singlets FSC-W/CD45) in combination with the pan-leukocyte marker. This refined population is then used for the downstream identification of T cells, B cells, and subsequent myeloid subsets, including the four step strategy for basophil identification.

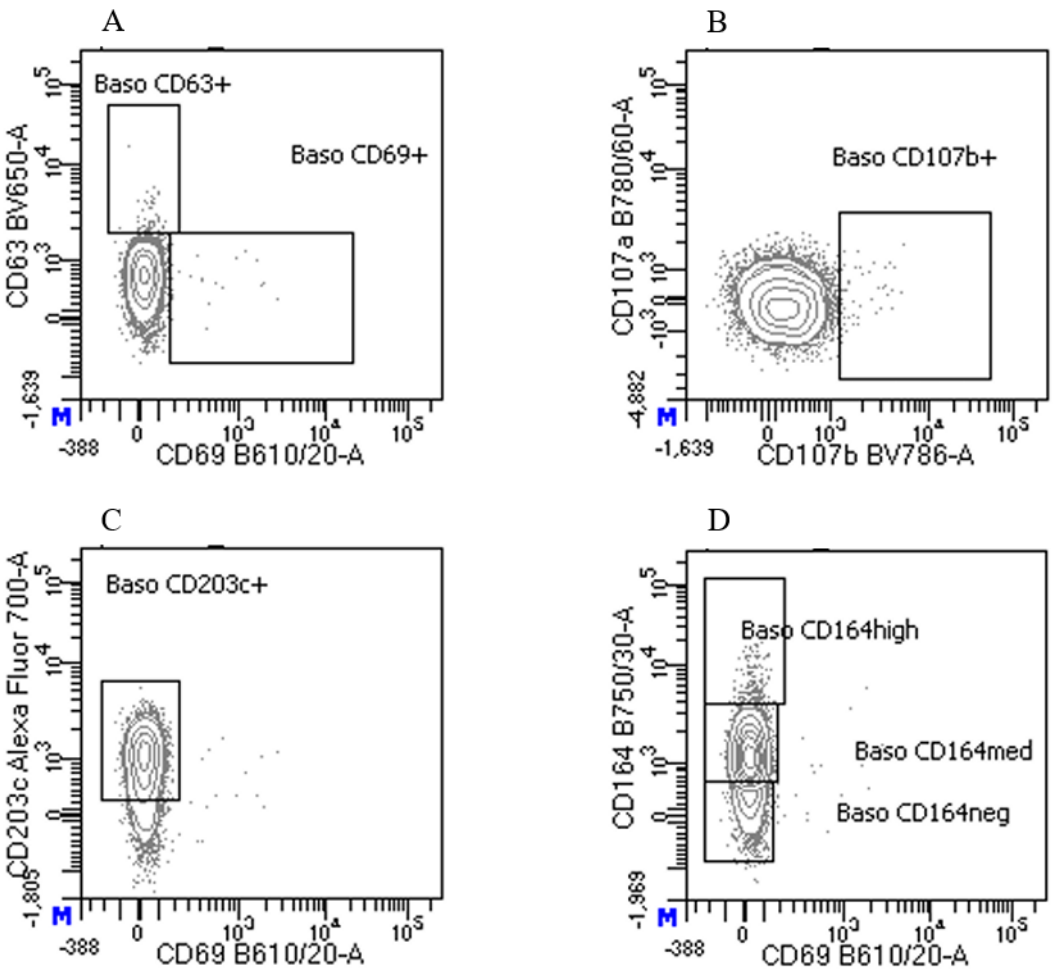

Figure 10: Functional characterization of basophil activation subsets. Representative flow cytometry contour plots showing the identification of seven distinct basophil subpopulations based on activation and degranulation markers. (**A**) Gating strategy for $CD63^{+}$ and $CD69^{+}$ activated basophils. (**B**) Identification of the $CD107b^{+}$ degranulating subset. (**C**) Selection of the $CD203c^{+}$ population. (**D**) Subclassification into $CD164^{neg}$, $CD164^{med}$, and $CD164^{high}$ basophils based on expression levels.

Discussion

ALS is a neurodegenerative disease of the adulthood, primarily distinguished by the progressive dysfunction of both LMN and UMN. While the underlying pathological mechanisms remain largely unknown, recent evidence has shifted the perspective of ALS towards a more systemic view of the disease. It's now clear that the immune system is involved in the pathology, although the neurotoxic or neuroprotective effects of different cellular populations remain to be fully elucidated. In this context, the alterations in the peripheral immune system represent a promising field for the identification of novel biomarkers to improve the diagnostic accuracy for ALS patients. To address this need, this study investigated immune differences between ALS patients and HC combining high-dimensional immunofluorescence staining of whole peripheral blood samples with unsupervised data analysis. Moreover, immune signatures were also investigated within the patient cohort, in order to identify possible prognostic biomarkers related to the progression rate of the pathology.

This study revealed increased basophils levels in ALS patients compared to HC. This finding is consistent with the work of Greco et al., who observed elevated basophil counts in blood samples from SP patients by leveraging a decade of longitudinal, routinely collected clinical data (Greco et al., 2021). Conversely, another study reported decreased basophils number, together with other alteration in the granulocytic compartment (Yang et al., 2023). Furthermore, in our study, specific cell clusters were associated here with clinical progression: while $CD4^+$ naïve T cells were decreased in SPs compared to FPs, basophils and classical monocytes were increased in SPs. Taken together, these results highlight the potential of specific immune signatures to act as both diagnostic and prognostic biomarkers.

Basophils are a type of innate immune cell primarily associated with allergic responses and parasitic infections. Through cytokine secretion, activated basophils are able to support the development of $CD4^+$ T cells and B cells secreting IgE, associated with the Th2 immune response (Chirumbolo, 2012). However, recent research has shed light on their potential roles in broader immune responses. Emerging studies highlight basophil involvement also in non-allergic and immune-mediated inflammatory diseases. A significant role of this cellular population has been observed in both local and systemic responses to atopic dermatitis. Upon rapid infiltration into inflamed skin, activated basophils release IL-4 and IL-13 alongside proinflammatory mediators like leukotrienes and IL-31, which collectively exacerbate tissue inflammation (Das & Geha, 2025). Moreover, according to the same study, basophil-derived IL-4 functions as a critical immunomodulator that directs T cell polarization and facilitates B cell class switching. In murine models, basophils facilitate TH17 cell differentiation via the secretion of IL-6. Consequently, in a neurodegenerative condition such as the

ALS, the depletion of basophils has been shown to ameliorate the clinical severity of experimental autoimmune encephalomyelitis (EAE), mouse model of multiple sclerosis (Yuk et al., 2017).

As stated previously, our study reported a significant increase in basophil levels in ALS patients compared to healthy controls, suggesting they may have a wider impact beyond allergy and parasitic infection. Although only in a preliminary form, an increased basophils number has been observed also in other pathological contexts, such as ulcerative colitis and Crohn disease (Badalyan et al., 2014). While in the aforementioned inflammatory or autoimmune diseases (such as atopic dermatitis or EAE) basophils often drive progression, in the context of ALS they might exert a more neuroprotective role, as supported by the higher basophil numbers that we observed in SPs. This protective role is possibly linked to histaminergic signaling. Genome-wide association studies have indicated that histamine-related genes may act as modifiers in ALS (Volonté et al., 2019), supporting the idea that both basophils and histaminergic pathways could serve as potential disease biomarkers and therapeutic targets. By interacting with astrocytes, histamine is able to inhibit glial scar formation and promote neurological function recovery, inhibiting neuroinflammation and participating in CNS homeostasis maintenance. (Zhou et al., 2024). Apolloni et al. have shown that histamine acts as an anti-inflammatory agent in microglia, suggesting that dysregulated this histaminergic signaling could have a detrimental effect in ALS (Apolloni et al., 2017; Mentis et al., 2021).

Besides the genetic background, environmental factors, such as infections, may play a role in ALS progression. Indeed, various parasite infections, including cerebral malaria, cerebral toxoplasmosis, and neurocysticercosis, have been associated with acute or chronic brain inflammation, leading to the disruption of the brain blood barrier and deregulation of glial activity. The resulting cytotoxic effect appears to be triggered by a substantial release of nitric oxide, oxygen reactive species, and pro-inflammatory mediators (Alloo et al., 2022). Moreover, David and colleagues have shown that Toxoplasma gondii infection in mouse models can disrupt CNS glutamate homeostasis by reducing GLT-1 transporters, leading to a robust increase in extracellular glutamate levels (David et al., 2016), which in turn may have a toxic effect on the CNS, potentially resulting in astrocyte death, a hallmark of ALS. We identify basophils as major contributors to the ALS immune profile, a phenomenon that may be ascribed to their classic role in mediating responses to parasitic threats. IL–3 is required for blood basophils expansion after parasitic infection. Moreover, the presence of IL–3 increases the in vitro IL–4 secretion from this cellular population (Lantz et al., 2008). Notably, the overexpression of IL–3 in transgenic models has been shown to induce motor neuron pathologies characterized by lower motor neuron deficits, further supporting a link between IL-3 signaling and the pathogenesis of ALS.

However, IL-3-treated MNs were affected neither in their survival nor in their differentiation, suggesting that the onset of symptoms does not result from a direct effect of IL–3 on motoneurons (Chavany et al., 1998).

While no major differences were noted between ALS patients and healthy controls, our findings also indicate a higher frequency of classical monocytes ($CD14^+$ $CD16^-$) in SPs compared to FPs. This cellular population is usually known to be pro-inflammatory. Recently, their anti-inflammatory potential has been recognized because of their ability to contribute to resolution of inflammation and tissue repair. In facts, while non-classical monocytes are more prone to differentiate into pro-resolutive $CD206^+$ M2 macrophages, classical monocytes are able to differentiate into both M1 and M2 macrophages (Olingy et al., 2017). More specifically, research has shown that these cells are recruited at the site of injury while possessing a pro-inflammatory state and later switch towards a more aini-inflammatory phenotype (Arnold et al., 2007). In our cohort, the increase in classical monocytes suggests a protective role of this population in ALS pathology, possibly linked with their anti-inflammatory ability. This hypothesis is in line with the study by Mantovani et al., which observed increased abundances of $CD14^+$ cells in earlier stages of ALS disease (Mantovani et al., 2009). Nonetheless, further functional studies are needed to clarify the mechanism of interactions.

Interestingly, an interaction between monocytes and basophils has been reported in other contexts, such as allergic responses. In particular, monocytes with an inflammatory phenotype are recruited to the site of inflammation and, reacting to basophil-derived IL–4, exert anti-inflammatory functions by differentiating into M2 macrophages (Egawa et al., 2013). The finding of both increased monocyte and basophil levels in ALS patients suggests that an interplay between these populations is possible also in context other than allergies. For this reason, we consider the analysis of these two populations a new approach that can help in better understanding ALS pathological mechanisms.

Another key finding is the increase in $CD4^+$ naïve T cells in FPs. These antigen-inexperienced cells are central to initiating immune responses and may reflect a heightened immune readiness. Paradoxically, this state could contribute to faster ALS progression by amplifying inflammation. On the other hand, this increased levels of $CD4^+$ naïve T cells may not be the results of an expansion of this cellular population, but a consequence of an impaired ability to differentiate of $CD4^+$ naïve T cells. Differences in the levels of expression of FoxP3 have been observed in ALS patients. In particular, low expression of this gene inversely correlate disease severity and progression rate (Henkel et al., 2013b). Fittingly, FoxP3 is required for differentiation of $CD4^+$ regulatory T cells. Considering that the neuroprotective effects of Treg cells has been observed in mouse models (Banerjee et al., 2008) and the abundance of these population has been negatively correlated with

disease progression (Mantovani et al., 2009; Rentzos et al., 2012; Henkel et al., 2013; Beers et al., 2017), it is possible that impaired differentiation determine both Treg decrease and CD4+ naïve T cells accumulation.

Given the prominent role of basophils emerged from our preliminary analysis, a deeper characterization of this population becomes essential. Therefore, the second part of this study focused on the design and optimization of a high-dimensional flow cytometry panel specifically tailored to dissect the basophil compartment, aiming to identify specific activation states or subsets associated with the different stages of ALS progression.

In the first phase, two hundred µL of whole blood were previously stained with antibodies and subsequently lysed to remove red blood cells. Instead, for the second phase, this approach was not suitable anymore because of the inclusion of an antibody directed against the IgE immunoglobulin within the immunofluorescence panel. IgE molecules are not exclusively present on the surface of the basophils compartment; they are also normally present at different concentration inside the blood flow in their circulating form and this can cause interference in the staining procedure if whole blood sample are used. In addition, basophils are the least abundant leukocyte population among peripheral blood cells, with standard physiological ranges between 0.5% and 1%. For this reason, the staining protocol has been partially modified in order to optimize it for the analysis of this rare population. Consequently, for the second phase of the study, 3.5 mL of whole blood were lysed prior to staining, and then 2 x 10^6 cells were subsequently used for the procedure. This approach allowed us to stain a significantly higher number of cells, facilitating the identification of different basophils subpopulation. Moreover, these modifications improved the standardization of the method, as a fixed number of cells were subjected to the staining procedure, regardless of the initial cell concentration in the whole blood.

Consistent with this tailored approach, the antibody panel was specifically designed and titrated for the staining of 2 x 10^6 cells. This setup was optimized to provide the high signal-to-noise ratio necessary for detecting precise functional markers within the basophil compartment. Markers such as CD3, CD19, and CD56 were used for lineage exclusion of respectively T cells, B cells and NK cells, while neutrophils and eosinophils granulocytes were excluded on the basis of their morphological characteristics. The rationale for CD14 and CD16 inclusion in the panel was twofold. On one hand, they were essential to the cleaning strategy for basophils identification, allowing for the exclusion of monocytes and residual neutrophils. On the other hand, these two markers enabled the characterization of different monocyte subpopulations, specifically classical ($CD14^+$ $CD16^-$), non-classical ($CD14^-$ $CD16^+$) and intermediate ($CD14^+$ $CD16^+$) monocytes.

Four specific markers were employed to accurately identify basophils: CD123, HLA–DR, IgE, and FcεRI (Sonder et al., 2023). From a technical standpoint, a rigorous sequential gating strategy based on multi-marker cross-validation was applied to ensure the highest possible phenotypic consistency and eliminate any potential contaminating populations. As illustrated in Figure 9, the basophil population was progressively refined through complementary marker combinations: HLA–DR^- / $FcεRI^+$, HLA–DR^- / $CD123^+$, and HLA–DR^- / IgE^+, ending with the selection of the $FcεRI^+$ / IgE^+ double-positive cells. Moreover, several activation and degranulation markers were included in the panel to classify this population from a functional perspective, as they are either unexpressed or weakly expressed on the surface of resting basophils.

In particular, CD203c is a basophil-specific marker, associated with histamine release, it is expressed in the resting basophils, but following activation is rapidly and significantly upregulated (Bühring et al., 2004). The same expression pattern is observed for CD13 and CD164, which normally reach the maximum expression level from five to fifteen minutes after basophil activation (Hennersdorf et al., 2005). A similar behavior, albeit with important differences, was observed for CD63. Indeed, this marker is highly upregulated following cellular activation, reaching a 100-fold increase compared to resting basophils. However, this event takes a longer time, with detectable CD63 levels observed after thirty minutes and a peak in expression reached after sixty minutes (Knol et al., 1991). A "CD63-like" regulation was observed also for CD107a and CD107b. Specifically, both these markers are upregulated in case of basophil activation, with CD107a reaching higher levels compared to its homologous counterpart (Hennersdorf et al., 2005). Together, these different markers can be analyzed to broadly investigate whether different basophil activation dynamics occur in ALS.

A third distinct behavior is observed for CD69. According to the work of Yoshimura and colleagues, the presence of this marker is low in resting basophils and significantly increases after IL-3 stimulation. However, the rate of increase is even slower when compared to the other previously mentioned, with complete expression reached only twenty-four hours after IL-3 induction. Even if the functional role of this marker is only partially understood, it demonstrated high biological relevance, with higher CD69 levels observed in basophils isolated from people affected by asthma (Yoshimura et al., 2002). For this reason, we decided nonetheless to include this marker in our panel, in order to evaluate a possible involvement in ALS pathology.

Lastly, CD244 was also included because of the recent advances in its localization and functional understanding. Compared to any other leukocytic population, a higher level of expression of this marker has been observed in basophils isolated from whole peripheral blood (Berger et al., 2021). Considering the functional role of CD244, it acts as a key regulator of immune homeostasis in autoimmune diseases and allergies, possessing the capacity to transmit both activating and inhibitory signals. In systemic lupus erythematosus (SLE), it exerts a negative regulatory role, and its downregulation exacerbates the pathology; conversely, in rheumatoid arthritis (RA) and allergic disorders, its overexpression drives detrimental inflammatory responses, such as TNF secretion and establishing the destructive crosstalk between eosinophils and mast cells (Sun et al., 2021). As previously noted, the first part of our study revealed that basophils were generally increased in ALS patients, a phenomenon that was particularly marked in SPs. This suggests a participation of this population in the underlying pathological mechanisms, potentially linked to a protective role regarding the rate of disease progression. We hypothesize that a thorough analysis of CD244 expression could provide crucial insights into the functional state of these cells. Given its dual, context-dependent activity, an upregulation of CD244 in SPs could mirror the protective, negative regulatory role observed in SLE, serving as an immunological brake against neuroinflammation. Conversely, a divergent mechanism in FPs cannot be excluded, where CD244 overexpression might instead drive detrimental inflammatory responses, akin to the patterns observed in rheumatoid arthritis and allergic disorders.

As a proof of concept, we used peripheral blood from a healthy donor (HD) to set up and validate the identification of these activation states. As shown in the Results section (Figure 10), this approach successfully allowed us to divide the total basophil population into seven distinct subsets based on the expression of CD63, CD69, CD107b, CD203c, and the three levels of CD164 (CD164neg, CD164med, and CD164high). Testing this panel on a healthy control was a necessary step before analyzing the ALS cohort, being able to clearly separate these seven subsets proves our panel sensitivity. This baseline characterization gives us the foundation to now investigate whether the frequencies or activation dynamics of these specific subsets are altered in ALS patients.

Despite the promising insights provided by this study, several limitations must be acknowledged. Firstly, despite the optimized high-dimensional approach combined with unsupervised analysis, the small size cohort (24 ALS patients, 15 HC) may reduce statistical power and generalizability. This is particularly impactful when patients are stratified according to different progression rate (SPs and FPs). Validation in a larger, multi-center cohort is required to confirm the robustness of these diagnostic and prognostic immune signatures. Secondly, the cross-sectional design of the study limits insight into dynamic immune changes over time. Longitudinal monitoring of the same individuals over multiple time points would provide a more precise understanding of how basophil abundances and their activation states dynamically shift as ALS progresses. Thirdly, focusing solely on immune cells may overlook other contributors to ALS progression. Moreover, this study in particular focuses exclusively on whole peripheral blood samples. While peripheral immune alterations represent excellent candidates for minimally invasive biomarkers, they may not fully or directly reflect the complex neuroinflammatory microenvironment.

Despite the limitations specified above, these findings open up several intriguing avenues for future research. Moving forward, the primary future direction will be to translate this newly optimized 22-color flow cytometry panel into a first clinical, exploratory study. This will allow us to evaluate the feasibility and technical reliability of the protocol when processing actual ALS patient samples. Secondly, this exploratory phase will be crucial to uncover whether significant differences in basophil subset are truly present between distinct patient subsets, providing the first direct experimental evidence of their dynamic involvement in ALS pathogenesis. Hopefully, this pilot study will lay the foundation for applying our newly designed panel to a larger and more substantial cohort of ALS patients.

Bibliography

Agosta, F., Al-Chalabi, A., Filippi, M., Hardiman, O., Kaji, R., Meininger, V., Nakano, I., Shaw, P., Shefner, J., Van Den Berg, L. H., & Ludolph, A. (2015). The El Escorial criteria: Strengths and weaknesses. *Amyotrophic Lateral Sclerosis and Frontotemporal Degeneration*, *16*(1–2), 1–7. https://doi.org/10.3109/21678421.2014.964258

Ahmed, R. M., Irish, M., Piguet, O., Halliday, G. M., Ittner, L. M., Farooqi, S., Hodges, J. R., & Kiernan, M. C. (2016). Amyotrophic lateral sclerosis and frontotemporal dementia: distinct and overlapping changes in eating behaviour and metabolism. In *The Lancet Neurology* (Vol. 15, Number 3, pp. 332–342). Lancet Publishing Group. https://doi.org/10.1016/S1474-4422(15)00380-4

Alloo, J., Leleu, I., Grangette, C., & Pied, S. (2022). Parasite infections, neuroinflammation, and potential contributions of gut microbiota. *Frontiers in Immunology*, *13*. https://doi.org/10.3389/fimmu.2022.1024998

Alshehri, R. S., Abuzinadah, A. R., Alrawaili, M. S., Alotaibi, M. K., Alsufyani, H. A., Alshanketi, R. M., & AlShareef, A. A. (2024). A Review of Biomarkers of Amyotrophic Lateral Sclerosis: A Pathophysiologic Approach. In *International Journal of Molecular Sciences* (Vol. 25, Number 20). Multidisciplinary Digital Publishing Institute (MDPI). https://doi.org/10.3390/ijms252010900

Apolloni, S., Fabbrizio, P., Amadio, S., Napoli, G., Verdile, V., Morello, G., Iemmolo, R., Aronica, E., Cavallaro, S., & Volonté, C. (2017). Histamine regulates the inflammatory profile of SOD1-G93A microglia and the histaminergic system is dysregulated in amyotrophic lateral sclerosis. *Frontiers in Immunology*, *8*(NOV). https://doi.org/10.3389/fimmu.2017.01689

Arnold, L., Henry, A., Poron, F., Baba-Amer, Y., Van Rooijen, N., Plonquet, A., Gherardi, R. K., & Chazaud, B. (2007). Inflammatory monocytes recruited after skeletal muscle injury switch into antiinflammatory macrophages to support myogenesis. *Journal of Experimental Medicine*, *204*(5), 1057–1069. https://doi.org/10.1084/jem.20070075

Badalyan, V., Thompson, R., Addo, K., Borthwick, L. A., Fisher, A. J., Ort, T., Myers, T. G., Wynn, T. A., & Ramalingam, T. R. (2014). Basophils increase in Crohn disease and ulcerative colitis and favor mesenteric lymph node memory TH17/TH1 response. *Journal of Allergy and Clinical Immunology*, *134*(4), 975-978.e5. https://doi.org/10.1016/j.jaci.2014.05.019

Banerjee, R., Mosley, R. L., Reynolds, A. D., Dhar, A., Jackson-Lewis, V., Gordon, P. H., Przedborski, S., & Gendelman, H. E. (2008). Adaptive immune neuroprotection in G93A-SOD1 amyotrophic lateral sclerosis mice. *PLoS ONE*, *3*(7). https://doi.org/10.1371/journal.pone.0002740

Beeldman, E., Govaarts, R., De Visser, M., Klein Twennaar, M., Van Der Kooi, A. J., Van Den Berg, L. H., Veldink, J. H., Pijnenburg, Y. A. L., De Haan, R. J., Schmand, B. A., & Raaphorst, J. (2020). Progression of cognitive and behavioural impairment in early amyotrophic lateral sclerosis. In *Journal of Neurology, Neurosurgery and Psychiatry* (Vol. 91, Number 7, pp. 779–780). BMJ Publishing Group. https://doi.org/10.1136/jnnp-2020-322992

Beers, D. R., Zhao, W., Wang, J., Zhang, X., Wen, S., Neal, D., Thonhoff, J. R., Alsuliman, A. S., Shpall, E. J., Rezvani, K., & Appel, S. H. (2017). ALS patients' regulatory T lymphocytes are dysfunctional, and correlate with disease progression rate and severity. *JCI Insight*, *2*(5). https://doi.org/10.1172/jci.insight.89530

Berger, A. E., Durrieu, C., Dzviga, C., Perrot, J. L., & Lambert, C. (2021). Human peripheral basophils extended phenotype shows a high expression of CD244 immuno-regulatory receptor. *Journal of Immunological Methods*, *492*. https://doi.org/10.1016/j.jim.2020.112951

Bjornevik, K., Munger, K. L., Cortese, M., Barro, C., Healy, B. C., Niebuhr, D. W., Scher, A. I., Kuhle, J., & Ascherio, A. (2020). Serum Neurofilament Light Chain Levels in Patients with Presymptomatic Multiple Sclerosis. *JAMA Neurology*, *77*(1), 58–64. https://doi.org/10.1001/jamaneurol.2019.3238

Bühring, H.-J., Streble, A., & Valent, P. (2004). The Basophil-Specific Ectoenzyme E-NPP3 (CD203c) as a Marker for Cell Activation and Allergy Diagnosis. *International Archives of Allergy and Immunology*, *133*(4), 317–329. https://doi.org/10.1159/000077351

Chavany, C., Vicario-Abejo´nabejo´n, C., Miller, G., & Jendoubi, M. (1998). Transgenic mice for interleukin 3 develop motor neuron degeneration associated with autoimmune reaction against spinal cord motor neurons. In *Medical Sciences* (Vol. 95). www.pnas.org.

Chiò, A., Calvo, A., Moglia, C., Mazzini, L., Mora, G., Mutani, R., Balma, M., Cammarosano, S., Canosa, A., Gallo, S., Ilardi, A., Durelli, L., Ferrero, B., De Mercanti, S., Mauro, A., Leone, M., Monaco, F., Nasuelli, N., Sosso, L., … Bottacchi, E. (2011). Phenotypic heterogeneity of amyotrophic lateral sclerosis: A population based study. *Journal of Neurology, Neurosurgery and Psychiatry*, *82*(7), 740–746. https://doi.org/10.1136/jnnp.2010.235952

Chirumbolo, S. (2012). State-of-the-art review about basophil research in immunology and allergy: Is the time right to treat these cells with the respect they deserve? In *Blood Transfusion* (Vol. 10, Number 2, pp. 148–164). https://doi.org/10.2450/2011.0020-11

Chiu, I. M., Chen, A., Zheng, Y., Kosaras, B., Tsiftsoglou, S. A., Vartanian, T. K., Brown, R. H. B., Carroll, M. C., & Day, B. (2008). *T lymphocytes potentiate endogenous neuroprotective inflammation in a mouse model of ALS*. www.pnas.orgcgidoi10.1073pnas.0804610105

Coque, E., Salsac, C., Espinosa-Carrasco, G., Varga, B., Degauque, N., Cadoux, M., Crabé, R., Virenque, A., Soulard, C., Fierle, J. K., Brodovitch, A., Libralato, M., Végh, A. G., Venteo, S., Scamps, F., Boucraut, J., Laplaud, D., Hernandez, J., Gergely, C., … Raoul, C. (2019). Cytotoxic CD8 + T lymphocytes expressing ALS-causing SOD1 mutant selectively trigger death of spinal motoneurons. *Proceedings of the National Academy of Sciences of the United States of America*, *116*(6), 2312–2317. https://doi.org/10.1073/pnas.1815961116

Crockford, C., Newton, J., Lonergan, K., Chiwera, T., Booth, T., Chandran, S., Colville, S., Heverin, M., Mays, I., Pal, S., Pender, N., Pinto-Grau, M., Radakovic, R., Shaw, C. E., Stephenson, L., Swingler, R., Vajda, A., Al-Chalabi, A., Hardiman, O., & Abrahams, S. (2018). ALS-specific cognitive and behavior changes associated with advancing disease stage in ALS. *Neurology*, *91*(15), E1370–E1380. https://doi.org/10.1212/WNL.0000000000006317

Das, M., & Geha, R. S. (2025). Basophils in atopic dermatitis. In *Annals of Allergy, Asthma and Immunology*. American College of Allergy, Asthma and Immunology. https://doi.org/10.1016/j.anai.2025.11.005

David, C. N., Frias, E. S., Szu, J. I., Vieira, P. A., Hubbard, J. A., Lovelace, J., Michael, M., Worth, D., McGovern, K. E., Ethell, I. M., Stanley, B. G., Korzus, E., Fiacco, T. A., Binder, D. K., & Wilson, E. H. (2016). GLT-1-Dependent Disruption of CNS Glutamate Homeostasis and Neuronal Function by the Protozoan Parasite Toxoplasma gondii. *PLoS Pathogens*, *12*(6). https://doi.org/10.1371/journal.ppat.1005643

Du, Y., Zhao, W., Thonhoff, J. R., Wang, J., Wen, S., & Appel, S. H. (2020). Increased activation ability of monocytes from ALS patients. *Experimental Neurology*, *328*. https://doi.org/10.1016/j.expneurol.2020.113259

Egawa, M., Mukai, K., Yoshikawa, S., Iki, M., Mukaida, N., Kawano, Y., Minegishi, Y., & Karasuyama, H. (2013). Inflammatory Monocytes Recruited to Allergic Skin Acquire an Anti-inflammatory M2 Phenotype via Basophil-Derived Interleukin-4. *Immunity*, *38*(3), 570–580. https://doi.org/10.1016/j.immuni.2012.11.014

Engelhardt, J. I., & Appel, S. H. (1990). IgG Reactivity in the Spinal Cord and Motor Cortex in Amyotrophic Lateral Sclerosis. *Archives of Neurology*, *47*(11), 1210–1216. https://doi.org/10.1001/archneur.1990.00530110068019

Finkelstein, A., Kunis, G., Seksenyan, A., Ronen, A., Berkutzki, T., Azoulay, D., Koronyo-Hamaoui, M., & Schwartz, M. (2011). Abnormal changes in NKT cells, the IGF-1 axis, and liver pathology in an animal model of ALS. *PLoS ONE*, *6*(8). https://doi.org/10.1371/journal.pone.0022374

Garofalo, S., Cocozza, G., Porzia, A., Inghilleri, M., Raspa, M., Scavizzi, F., Aronica, E., Bernardini, G., Peng, L., Ransohoff, R. M., Santoni, A., & Limatola, C. (2020). Natural killer cells modulate motor neuron-immune cell cross talk in models of Amyotrophic Lateral Sclerosis. *Nature Communications*, *11*(1). https://doi.org/10.1038/s41467-020-15644-8

Geevasinga, N., Loy, C. T., Menon, P., de Carvalho, M., Swash, M., Schrooten, M., Van Damme, P., Gawel, M., Sonoo, M., Higashihara, M., Noto, Y. ichi, Kuwabara, S., Kiernan, M. C., Macaskill, P., & Vucic, S. (2016). Awaji criteria improves the diagnostic sensitivity in amyotrophic lateral sclerosis: A systematic review using individual patient data. *Clinical Neurophysiology*, *127*(7), 2684–2691. https://doi.org/10.1016/j.clinph.2016.04.005

Goutman, S. A., Hardiman, O., Al-Chalabi, A., Chió, A., Savelieff, M. G., Kiernan, M. C., & Feldman, E. L. (2022a). Emerging insights into the complex genetics and pathophysiology of amyotrophic lateral sclerosis. *The Lancet Neurology*, *21*(5), 465–479. https://doi.org/10.1016/S1474-4422(21)00414-2

Goutman, S. A., Hardiman, O., Al-Chalabi, A., Chió, A., Savelieff, M. G., Kiernan, M. C., & Feldman, E. L. (2022b). Recent advances in the diagnosis and prognosis of amyotrophic lateral sclerosis. In *The Lancet Neurology* (Vol. 21, Number 5, pp. 480–493). Elsevier Ltd. https://doi.org/10.1016/S1474-4422(21)00465-8

Greco, A., Chiesa, M. R., Da Prato, I., Romanelli, A. M., Dolciotti, C., Cavallini, G., Masciandaro, S. M., Scilingo, E. P., Del Carratore, R., & Bongioanni, P. (2021). Using blood data for the differential diagnosis and prognosis of motor neuron diseases: a new dataset for machine learning applications. *Scientific Reports*, *11*(1). https://doi.org/10.1038/s41598-021-82940-8

Gustafson, M. P., Staff, N. P., Bornschlegl, S., Butler, G. W., Maas, M. L., Kazamel, M., Zubair, A., Gastineau, D. A., Windebank, A. J., & Dietz, A. B. (2017). Comprehensive immune profiling reveals substantial immune system alterations in a subset of patients with amyotrophic lateral sclerosis. *PLoS ONE*, *12*(7). https://doi.org/10.1371/journal.pone.0182002

Henkel, J. S., Beers, D. R., Wen, S., Rivera, A. L., Toennis, K. M., Appel, J. E., Zhao, W., Moore, D. H., Powell, S. Z., & Appel, S. H. (2013a). Regulatory T-lymphocytes mediate amyotrophic lateral sclerosis progression and survival. *EMBO Molecular Medicine*, *5*(1), 64–79. https://doi.org/10.1002/emmm.201201544

Henkel, J. S., Beers, D. R., Wen, S., Rivera, A. L., Toennis, K. M., Appel, J. E., Zhao, W., Moore, D. H., Powell, S. Z., & Appel, S. H. (2013b). Regulatory T-lymphocytes mediate amyotrophic lateral sclerosis progression and survival. *EMBO Molecular Medicine*, *5*(1), 64–79. https://doi.org/10.1002/emmm.201201544

Hennersdorf, F., Florian, S., Jakob, A., Baumgärtner, K., Sonneck, K., Nordheim, A., Biedermann, T., Valent, P., & Bühring, H.-J. (2005). Identification of CD13, CD107a, and CD164 as novel basophil-activation markers and dissection of two response patterns in time kinetics of IgE-de-pendent upregulation. In *Cell Research* (Vol. 15, Number 5). www.cell-research.com

Hu, Y., Chen, W., Wei, C., Jiang, S., Li, S., Wang, X., & Xu, R. (2024b). Pathological mechanisms of amyotrophic lateral sclerosis. In *Neural Regeneration Research* (Vol. 19, Number 5, pp. 1036–1044). Wolters Kluwer Medknow Publications. https://doi.org/10.4103/1673-5374.382985

Jin, M., Günther, R., Akgün, K., Hermann, A., & Ziemssen, T. (2020). Peripheral proinflammatory Th1/Th17 immune cell shift is linked to disease severity in amyotrophic lateral sclerosis. *Scientific Reports*, *10*(1). https://doi.org/10.1038/s41598-020-62756-8

Kim, Z., Choi, B. S., Kim, J. K., & Won, D. Il. (2016). Basophil markers for identification and activation in the indirect basophil activation test by flow cytometry for diagnosis of autoimmune urticaria. *Annals of Laboratory Medicine*, *36*(1), 28–35. https://doi.org/10.3343/alm.2016.36.1.28

Knol, E. F., Mul, F. P. J., Jansen, H., Calafat, J., & Roos, D. (1991). Monitoring human basophil activation via CD63 monoclonal antibody 435. *Journal of Allergy and Clinical Immunology*, *88*(3), 328–338. https://doi.org/10.1016/0091-6749(91)90094-5

Lantz, C. S., Min, B., Tsai, M., Chatterjea, D., Dranoff, G., & Galli, S. J. (2008). IL-3 is required for increases in blood basophils in nematode infection in mice and can enhance IgE-dependent IL-4 production by basophils in vitro. *Laboratory Investigation*, *88*(11), 1134–1142. https://doi.org/10.1038/labinvest.2008.88

Mantovani, S., Garbelli, S., Pasini, A., Alimonti, D., Perotti, C., Melazzini, M., Bendotti, C., & Mora, G. (2009). Immune system alterations in sporadic amyotrophic lateral sclerosis patients suggest an ongoing neuroinflammatory process. *Journal of Neuroimmunology*, *210*(1–2), 73–79. https://doi.org/10.1016/j.jneuroim.2009.02.012

May, C., Nordhoff, E., Casjens, S., Turewicz, M., Eisenacher, M., Gold, R., Brüning, T., Pesch, B., Stephan, C., Woitalla, D., Penke, B., Janáky, T., Virók, D., Siklós, L., Engelhardt, J. I., & Meyer, H. E. (2014). Highly immunoreactive IgG antibodies directed against a set of twenty human proteins in the sera of patients with amyotrophic lateral sclerosis identified by protein array. *PLoS ONE*, *9*(2). https://doi.org/10.1371/journal.pone.0089596

Mentis, A. F. A., Bougea, A. M., & Chrousos, G. P. (2021). Amyotrophic lateral sclerosis (ALS) and the endocrine system: Are there any further ties to be explored? In *Aging Brain* (Vol. 1). Elsevier Inc. https://doi.org/10.1016/j.nbas.2021.100024

Münch, M., Müller, H. P., Behler, A., Ludolph, A. C., & Kassubek, J. (2022). Segmental alterations of the corpus callosum in motor neuron disease: A DTI and texture analysis in 575 patients. *NeuroImage: Clinical*, *35*. https://doi.org/10.1016/j.nicl.2022.103061

Munitz, A., Bachelet, I., Fraenkel, S., Katz, G., Mandelboim, O., Simon, H.-U., Moretta, L., Colonna, M., & Levi-Schaffer, F. (2005). *2B4 (CD244) Is Expressed and Functional on Human Eosinophils1*. https://academic.oup.com/jimmunol/article/174/1/110/8036524

Murdock, B. J., Bender, D. E., Kashlan, S. R., Figueroa-Romero, C., Backus, C., Callaghan, B. C., Goutman, S. A., & Feldman, E. L. (2016). Increased ratio of circulating neutrophils to monocytes in amyotrophic lateral sclerosis. *Neurology: Neuroimmunology and NeuroInflammation*, *3*(4). https://doi.org/10.1212/NXI.0000000000000242

Murdock, B. J., Famie, J. P., Piecuch, C. E., Pawlowski, K. D., Mendelson, F. E., Pieroni, C. H., Iniguez, S. D., Zhao, L., Goutman, S. A., & Feldman, E. L. (2021). *NK cells associate with ALS in a sex-and age-dependent manner*. https://doi.org/10.1172/jci

Murdock, B. J., Zhou, T., Kashlan, S. R., Little, R. J., Goutman, S. A., & Feldman, E. L. (2017). Correlation of peripheral immunity with rapid Amyotrophic lateral sclerosis progression. *JAMA Neurology*, *74*(12), 1446–1454. https://doi.org/10.1001/jamaneurol.2017.2255

Naor, S., Keren, Z., Bronshtein, T., Goren, E., MacHluf, M., & Melamed, D. (2009). Development of ALS-like disease in SOD-1 mice deficient of B lymphocytes. *Journal of Neurology*, *256*(8), 1228–1235. https://doi.org/10.1007/s00415-009-5097-3

Neumann, M., Sampathu, D. M., Kwong, L. K., Truax, A. C., Micsenyi, M. C., Chou, T. T., Bruce, J., Schuck, T., Grossman, M., Clark, C. M., McCluskey, L. F., Miller, B. L., Masliah, E., Mackenzie, I. R., Feldman, H., Feiden, W., Kretzschmar, H. A., Trojanowski, J. Q., & M-Y Lee, V. (n.d.). *Ubiquitinated TDP-43 in Frontotemporal Lobar Degeneration and Amyotrophic Lateral Sclerosis*. Retrieved https://www.science.org

Obál, I., Nógrádi, B., Meszlényi, V., Patai, R., Ricken, G., Kovacs, G. G., Tripolszki, K., Széll, M., Siklós, L., & Engelhardt, J. I. (2019). Experimental motor neuron disease induced in mice with long-term repeated intraperitoneal injections of serum from ALS patients. *International Journal of Molecular Sciences*, *20*(10). https://doi.org/10.3390/ijms20102573

Olingy, C. E., San Emeterio, C. L., Ogle, M. E., Krieger, J. R., Bruce, A. C., Pfau, D. D., Jordan, B. T., Peirce, S. M., & Botchwey, E. A. (2017). Non-classical monocytes are biased progenitors of wound healing macrophages during soft tissue injury. *Scientific Reports*, *7*(1). https://doi.org/10.1038/s41598-017-00477-1

Pan, Y., & Nicolazzo, J. A. (2022). Altered blood–brain barrier and blood–spinal cord barrier dynamics in amyotrophic lateral sclerosis: Impact on medication efficacy and safety. In *British Journal of Pharmacology* (Vol. 179, Number 11, pp. 2577–2588). John Wiley and Sons Inc. https://doi.org/10.1111/bph.15802

Preische, O., Schultz, S. A., Apel, A., Kuhle, J., Kaeser, S. A., Barro, C., Gräber, S., Kuder-Buletta, E., LaFougere, C., Laske, C., Vöglein, J., Levin, J., Masters, C., Martins, R., Schofield, P., Rossor, M. N., Graff-Radford, N., Salloway, S., Ghetti, B., … Xu, X. (2019). Serum neurofilament dynamics predicts neurodegeneration and clinical progression in presymptomatic Alzheimer's disease. *Nature Medicine*, *25*(2), 277–283. https://doi.org/10.1038/s41591-018-0304-3

Rentzos, M., Evangelopoulos, E., Sereti, E., Zouvelou, V., Marmara, S., Alexakis, T., & Evdokimidis, I. (2012). Alterations of T cell subsets in ALS: A systemic immune activation? *Acta Neurologica Scandinavica*, *125*(4), 260–264. https://doi.org/10.1111/j.1600-0404.2011.01528.x

Robberecht, W., & Philips, T. (2011). Neuroinfl ammation in amyotrophic lateral sclerosis: role of glial activation in motor neuron disease. In *Lancet Neurol* (Vol. 10). www.thelancet.com/

Saleh, I. A., Zesiewicz, T., Xie, Y., Sullivan, K. L., Miller, A. M., Kuzmin-Nichols, N., Sanberg, P. R., & Garbuzova-Davis, S. (2009). Evaluation of humoral immune response in adaptive immunity in ALS patients during disease progression. *Journal of Neuroimmunology*, *215*(1–2), 96–101. https://doi.org/10.1016/J.JNEUROIM.2009.07.011

Shepheard, S. R., Karnaros, V., Benyamin, B., Schultz, D. W., Dubowsky, M., Wuu, J., Chataway, T., Malaspina, A., Benatar, M., & Rogers, M. L. (2022). Urinary neopterin: A novel biomarker of disease progression in amyotrophic lateral sclerosis. *European Journal of Neurology*, *29*(4), 990–999. https://doi.org/10.1111/ene.15237

Sonder, S. U., Plassmeyer, M., Loizou, D., & Alpan, O. (2023). Towards standardizing basophil identification by flow cytometry. *Frontiers in Allergy*, *4*. https://doi.org/10.3389/falgy.2023.1133378

Strong, M. J., Abrahams, S., Goldstein, L. H., Woolley, S., Mclaughlin, P., Snowden, J., Mioshi, E., Roberts-South, A., Benatar, M., HortobáGyi, T., Rosenfeld, J., Silani, V., Ince, P. G., & Turner, M. R. (2017). Amyotrophic lateral sclerosis - frontotemporal spectrum disorder (ALS-FTSD): Revised diagnostic criteria. *Amyotrophic Lateral Sclerosis and Frontotemporal Degeneration*, *18*(3–4), 153–174. https://doi.org/10.1080/21678421.2016.1267768

Sun, L., Gang, X., Li, Z., Zhao, X., Zhou, T., Zhang, S., & Wang, G. (2021). Advances in Understanding the Roles of CD244 (SLAMF4) in Immune Regulation and Associated Diseases. In *Frontiers in Immunology* (Vol. 12). Frontiers Media S.A. https://doi.org/10.3389/fimmu.2021.648182

Trias, E., King, P. H., Si, Y., Kwon, Y., Varela, V., Ibarburu, S., Kovacs, M., Moura, I. C., Beckman, J. S., Hermine, O., & Barbeito, L. (2018). Mast cells and neutrophils mediate peripheral motor pathway degeneration in ALS. *JCI Insight*, *3*(19). https://doi.org/10.1172/jci.insight.123249

Troost D, van den Oord JJ, de Jong JM, Swaab DF. Lymphocytic infiltration in the spinal cord of patients with amyotrophic lateral sclerosis. Clin Neuropathol. 1989 Nov-Dec;8(6):289-94. PMID: 2533530.

van den Bos, M. A. J., Geevasinga, N., Higashihara, M., Menon, P., & Vucic, S. (2019). Pathophysiology and diagnosis of ALS: Insights from advances in neurophysiological techniques. In *International Journal of Molecular Sciences* (Vol. 20, Number 11). MDPI AG. https://doi.org/10.3390/ijms20112818

Van Harten, A. C. M., Phatnani, H., & Przedborski, S. (2021). Non-cell-autonomous pathogenic mechanisms in amyotrophic lateral sclerosis. In *Trends in Neurosciences* (Vol. 44, Number 8, pp. 658–668). Elsevier Ltd. https://doi.org/10.1016/j.tins.2021.04.008

Volonté, C., Apolloni, S., & Sabatelli, M. (2019). Histamine beyond its effects on allergy: Potential therapeutic benefits for the treatment of Amyotrophic Lateral Sclerosis (ALS). In *Pharmacology and Therapeutics* (Vol. 202, pp. 120–131). Elsevier Inc. https://doi.org/10.1016/j.pharmthera.2019.06.006

Vu, L., An, J., Kovalik, T., Gendron, T., Petrucelli, L., & Bowser, R. (2020). Cross-sectional and longitudinal measures of chitinase proteins in amyotrophic lateral sclerosis and expression of CHI3L1 in activated astrocytes. *Journal of Neurology, Neurosurgery and Psychiatry*, *91*(4), 350–358. https://doi.org/10.1136/jnnp-2019-321916

Vucic, S., Ferguson, T. A., Cummings, C., Hotchkin, M. T., Genge, A., Glanzman, R., Roet, K. C. D., Cudkowicz, M., & Kiernan, M. C. (2021). Gold Coast diagnostic criteria: Implications for ALS diagnosis and clinical trial enrollment. *Muscle and Nerve*, *64*(5), 532–537. https://doi.org/10.1002/mus.27392

Witzel, S., Wagner, M., Zhao, C., Kandler, K., Graf, E., Berutti, R., Oexle, K., Brenner, D., Winkelmann, J., & Ludolph, A. C. (2022). Fast versus slow disease progression in amyotrophic lateral sclerosis–clinical and genetic factors at the edges of the survival spectrum. *Neurobiology of Aging*, *119*, 117–126. https://doi.org/10.1016/j.neurobiolaging.2022.07.005

Yang, J., Liu, T., Zhang, L., Li, X., Du, F. P., Liu, Q., Dong, H., & Liu, Y. (2023). Eosinophils at diagnosis are elevated in amyotrophic lateral sclerosis. *Frontiers in Neurology*, *14*. https://doi.org/10.3389/fneur.2023.1289467

Yoshimura, C., Yamaguchi, M., Iikura, M., Izumi, S., Kudo, K., Nagase, H., Ishii, A., Walls, A. F., Ra, C., Iwata, T., Igarashi, T., Yamamoto, K., & Hirai, K. (2002). Activation markers of human basophils: CD69 expression is strongly and preferentially induced by IL-3. *Journal of Allergy and Clinical Immunology*, *109*(5), 817–823. https://doi.org/10.1067/mai.2002.123532

Yuk, C. M., Park, H. J., Kwon, B. I., Lah, S. J., Chang, J., Kim, J. Y., Lee, K. M., Park, S. H., Hong, S., & Lee, S. H. (2017). Basophil-derived IL-6 regulates TH17 cell differentiation and CD4 T cell immunity. *Scientific Reports*, *7*. https://doi.org/10.1038/srep41744

Zecca, C., Dell'Abate, M. T., Pasculli, G., Capozzo, R., Barone, R., Arima, S., Pollice, A., Brescia, V., Tortelli, R., & Logroscino, G. (2022). Role of plasma phosphorylated neurofilament heavy chain (pNfH) in amyotrophic lateral sclerosis. *Journal of Cellular and Molecular Medicine*, *26*(13), 3608–3615. https://doi.org/10.1111/jcmm.17232

Zhang, R., Gascon, R., Miller, R. G., Gelinas, D. F., Mass, J., Hadlock, K., Jin, X., Reis, J., Narvaez, A., & McGrath, M. S. (2005). Evidence for systemic immune system alterations in sporadic amyotrophic lateral sclerosis (sALS). *Journal of Neuroimmunology*, *159*(1–2), 215–224. https://doi.org/10.1016/j.jneuroim.2004.10.009

Zhao, W., Beers, D. R., Hooten, K. G., Sieglaff, D. H., Zhang, A., Kalyana-Sundaram, S., Traini, C. M., Halsey, W. S., Hughes, A. M., Sathe, G. M., Livi, G. P., Fan, G. H., & Appel, S. H. (2017). Characterization of gene expression phenotype in amyotrophic lateral sclerosis monocytes. *JAMA Neurology*, *74*(6), 677–685. https://doi.org/10.1001/jamaneurol.2017.0357

Zhou, Z., An, Q., Zhang, W., Li, Y., Zhang, Q., & Yan, H. (2024). Histamine and receptors in neuroinflammation: Their roles on neurodegenerative diseases. In *Behavioural Brain Research* (Vol. 465). Elsevier B.V. https://doi.org/10.1016/j.bbr.2024.114964

Zondler, L., Müller, K., Khalaji, S., Bliederhäuser, C., Ruf, W. P., Grozdanov, V., Thiemann, M., Fundel-Clemes, K., Freischmidt, A., Holzmann, K., Strobel, B., Weydt, P., Witting, A., Thal, D. R., Helferich, A. M., Hengerer, B., Gottschalk, K. E., Hill, O., Kluge, M., … Weishaupt, J. H. (2016). Peripheral monocytes are functionally altered and invade the CNS in ALS patients. *Acta Neuropathologica*, *132*(3), 391–411. https://doi.org/10.1007/s00401-016-1548-y

Zucchi, E., Lu, C. H., Cho, Y., Chang, R., Adiutori, R., Zubiri, I., Ceroni, M., Cereda, C., Pansarasa, O., Greensmith, L., Malaspina, A., & Petzold, A. (2018). A motor neuron strategy to save time and energy in neurodegeneration: adaptive protein stoichiometry. *Journal of Neurochemistry*, *146*(5), 631–641. https://doi.org/10.1111/jnc.14542

Acknowledgment

During the preparation of this work the authors used Gemini/Google in order to improve the readability and language of the manuscript. After using this tool/service, the authors reviewed and edited the content as needed and take full responsibility for the content of the work.